A STUDY OF PARAMETERS INFLUENCING THE VEHICLE WHEEL
ALIGNMENT MEASUREMENTS.

by

Harsh H. Patel

A thesis submitted to the faculty of
The University of North Carolina at Charlotte
in partial fulfillment of the requirements
for the degree of Master of Science in
Mechanical Engineering

Charlotte

2016

Approved by:

_____

Dr. Peter T. Tkacik

_____

Dr. Mesbah Uddin

_____

Dr. Jimmie A. Miller

ABSTRACT

HARSH H. PATEL. A study of parameters influencing the vehicle wheel alignment measurements.
(Under the direction of DR. PETER T. TKACIK)

This research effort includes hundreds of passenger vehicle wheel alignment measurements and a design of experiments that works to capture the various factors influencing wheel alignment measurements. Of the many things that influence the accuracy and repeatability of vehicle suspension alignment measurement and adjustment, the design of the suspension can be the most significant. This includes but is not limited to adjustment configuration, suspension design, static alignment settings, and bushing stiffness.

Measurements were taken using a Hunter Pro-Align with DSP700 wheel sensors in the Motorsports Research Building at the University of North Carolina at Charlotte. All vehicles were reviewed and any with suspension damage were rejected prior to measurement. The collection of vehicles measured included the category of small front wheel drive, full size rear drive, seven passenger SUV, sports car, and race car. A small sporty sedan was also tested and modified to assess bushing stiffness influence.

Accuracy of the equipment is not a significant part of this study since after a strong attempt to measure it, we were not able to achieve measurements that could sense any reasonable measurement errors. The equipment seems to measure to the 0.01° resolution that it claims. Repeatability was evaluated by performing repeated measurements on the same day, a week apart, and over several months. Typically, ten repeats were made during each session and the standard deviation was compared.

The majority of the variability in suspension adjustment and measurement was determined to be from the stiffness (or lack thereof) of the suspension and its bushings. This was found to be the case even for static suspension settings far from the norm.

The NASCAR race car with its +6° left front (LF) camber had some of the lowest variation in the whole test.

DEDICATION

I dedicate my thesis work to my family and friends. A special feeling of gratitude to my loving parents, Hitesh and Nisha Patel for their continuous support throughout my career.

I also dedicate this thesis to my grandparents, my uncles Sanjay and Hemant Patel, my aunts Bhavina and Chaitali Patel for their unconditional love and support which motivated me to set higher targets.

A special thanks to my cousins Kesha, Parth and Aksh who have never left my side and are very special.

ACKNOWLEDGEMENTS

TABLE OF CONTENTS

LIST OF FIGURES

LIST OF TABLES

CHAPTER 1:   INTRODUCTION

1.1   Wheel Alignment

The tire is the only contact between the vehicle and the road. It serves as a transfer mechanism for forces between the vehicle and the road. From a vehicle dynamics point of view, the alignment of the wheels is of utmost importance. The kinematics and the kinetics of the suspension system in a vehicle is largely governed by the alignment of the wheels. Tire alignment, also known as wheel alignment, can help your tires perform properly and help them last longer. It can also improve handling and keep your vehicle from pulling in one direction or vibrating abnormally on the road. Alignment refers to an adjustment of a vehicle's suspension attachments that connect a vehicle to its wheels. It is not an adjustment of the tires or wheels themselves. The key to proper alignment is adjusting the angles of the tires which affects how they make contact with the road. The purpose of these adjustments is to reduce tire wear, and to ensure that vehicle travel is straight and true (without "pulling" to one side). Alignment angles can also be altered beyond the maker's specifications to obtain a specific handling characteristic. Motorsport and off-road applications may call for angles to be adjusted well beyond "normal" for a variety of reasons. Wheel alignment, hence, is a primary aspect in the field of vehicle dynamics.

1.2   Motivation

Vehicle wheel alignments that are so time consuming in the automobile assembly process are critical to optimum vehicle performance yet the accuracy of its measurement equipment and operator is not very well characterized. Since wheel alignment can be the bottle neck in production, automobile manufacturers have great interest in

speeding up the assembly line process and many things influence the measurement of vehicle wheel alignment including the alignment equipment, suspension design, and operator protocols [1]. Wheel alignment technicians are called on to provide accurate measurements; however, if some protocols slow down a measurement, pressure may be on the technician to take short cuts. Some of these may be trivial and some are shown to be very sensitive. The alignment of the suspension components can be faulty due to inconsistencies in testing methods and setup of the test equipment, variability in vehicle suspension components and inconsistencies in wheel alignment equipment measurements. Proper alignment of your vehicles wheels, front and back, is critical for safety and a very important part of vehicle maintenance. Even if the vehicle has not met an accident, its still worth having your vehicle alignment checked regularly, since improper alignment can affect vehicle handling and tire wear.

The aim of this research is to look into many of various influential effects on the alignment measurement. Variables studied include such things as jouncing the vehicle (bouncing it up and down to minimize suspension stiction), allowance of binding in the bearing plates, properly centering of the alignment head, and properly compensating the angular correction of the alignment heads. Of the many things that influence the accuracy and repeatability of vehicle suspension alignment measurement and adjustment, the design of the suspension can be the most significant. This includes but is not limited to adjustment configuration, spring preload (wedge), suspension design, static alignment settings, and bushing stiffness. For this research, a full vehicle alignment measurement included camber and toe-in for the left front (LF), RF, LR, and RR wheels. Caster sweeps were also performed, (typically a +17° to -17° steer sweep for both front tires) [2]. The alignment equipment in this research has been tuned and adjusted to minimize external variables and 300+ vehicle measurements were done. Influence of these variables on the suspension parameters camber, caster and toe variation are presented. This research will serve as a good platform for im-

provement in design of vehicle suspensions designs, wheel alignment equipment and wheel alignment procedures.

1.3 Organization of Thesis

Chapter 1 gives a brief introduction to wheel alignment and indicates the motivation for this thesis.

Chapter 2 presents the different types of wheel alignment methods and the working of the wheel alignment equipment used for research. A background of vehicle suspension system with its different types and suspension bushings is explained.

Chapter 3 includes test protocol and procedure followed throughout the research. It also gives a glimpse about measurement of bushing stiffness and details about the tensile testing machine used to measure the bushing stiffness.

Chapter 4 enlists the results of the research with conclusion and future scope.

CHAPTER 2:   LITERATURE REVIEW

2.1   Introduction

On the basis suspension geometry and design, wheel alignment can be classified into three major types: front-end, thrust and four-wheel. Each of these can be further classified into mechanical and computerized based on the applications and the accuracy required in setup. Their descriptions follow in subsequent sections under Section 2.5. The basics of different suspension types, suspension geometry and suspension angles related to wheel alignment are covered in Section 2.2. The background about suspension stiffness and suspension bushings is explained in Sections 2.3 and 2.4. A detailed description about the working principle of the wheel alignment machine used for this research is covered in Section 2.6.

2.2   Vehicle Suspension System

2.2.1   History of Vehicle Suspension System

Centuries ago the vehicle suspension was composed of a single solid axle which was pivoted in the center and attached to the horse in the front.

Front View
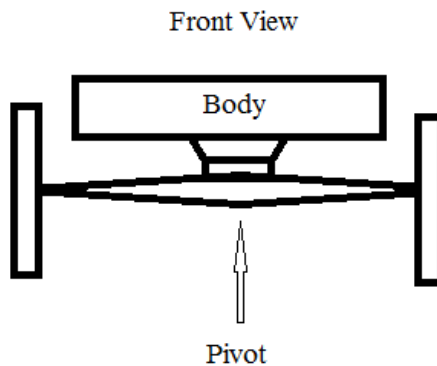
Figure 2.1: Single pivot front axle [3].

The power and the direction of the front wheels to the vehicle was supplied by the horse. The suspension system consisted of four flexible leaf-springs placed in four corners. In those days, the drivers had bigger problems to worry about instead of worrying about the suspension problems or comfort. Keeping the vehicle stable over big stones and potholes on the road was a matter of importance. Also braking was a problem since any imbalance in side-side braking would affect the stability of the vehicle. Later the Ackerman axle came into existence replacing the single pivoted solid axle by the Ackerman axle. The Ackerman axle was fixed and the steering took place through two pivot points, one on each end of the axle which are connected by kingpins. The vehicle suspension since then changed continuously from the Ackerman axle to the Elliot axle, then to the Reverse Elliot axle [3].

As more and more research was carried out on suspension design, it was learned that the ride smoothness or comfort was dependent on unsprung mass. In other words, the mass which was not supported by the springs (wheels, brakes, tires, suspension parts, etc.) was large, the ride smoothness would be lower. Solid straight axles were too heavy and thus dominated the unsprung mass. Thus, due to poor handling characteristics and vehicle instability there was a need for a new design, which led to modern suspension design with complex control algorithms [3].

The suspension system is a link between the vehicle chassis and the wheels. Suspension systems are designed to provide ride comfort, road contact and proper handling. The basic principles of any suspension system are [4]:-

1. Light weight components especially unsprung mass which affect vehicle handling.

2. Minimal roll and pitch of the vehicle from suitable design and attachment of springs.

3. To absorb small and large impacts with the assistance of and dampers.

2.2.2   Types of Suspension Systems

Over the years, researchers have set out to improve handling with different types of suspension for both front and rear axles. The suspension systems are divided into two main categories - beam axle and independent suspension. Since most of the independent suspensions are joined across by an anti-roll bar, they are not truly independent. The different types of suspensions used on the cars tested for this research are explained in the following sections.

2.2.2.1   MacPherson Strut Suspension

The MacPherson Strut is the most widely used front suspension system because of its simplicity itself. This suspension was first designed by a GM engineer Earle S. MacPherson [5]. The system is comprised of a strut type spring and shock absorber, which is attached to the lower control arm using a ball joint. The strut is the only load bearing member in the assembly, with the shock absorber and spring actually hold the car up. In figure 2.2 the shock absorber is hidden because it is inside the spring.

Figure 2.2: MacPherson Strut suspension [6].

The steering gear is either connected directly to an arm or lower shock absorber housing, or back of the spindle. While steering the vehicle, the strut and shock absorber are twisted physically to turn the wheel. The special plate at the top of the

assembly is where the spring is seated and has a bearing to allow twisting. The single lower control arm controls the lateral and longitudinal location of the wheel.

2.2.2.2   Double Wishbone Suspension

The double wishbone suspension also known as Double A-arm suspension because of its 'A' shaped arms. It consists of two A-shaped arms called as upper and lower A-arms which support the wheel spindle. as shown in figure 2.3 the spring and damper maybe attached to the lower control arm,and most of the vehicle load is carried by the lower arm [10]. In the front view, the arms form a parallelogram system which allows the spindle to travel up and down. During this vertical motion, they have a small side-to-side motion called scrub due to the arc subtended by the wishbones from their pivot points. When the suspension articulates, there are two types of motion of the wheel relative to the body. The first is steer angle which is most important and the second is camber angle which is least important. Double wishbone suspensions typically have shorter upper A-arms that provide increased negative camber on jounce. This partially compensates for vehicle body roll. This camber compensation is typically only 50% of body roll and referred to as "50% camber compensation".
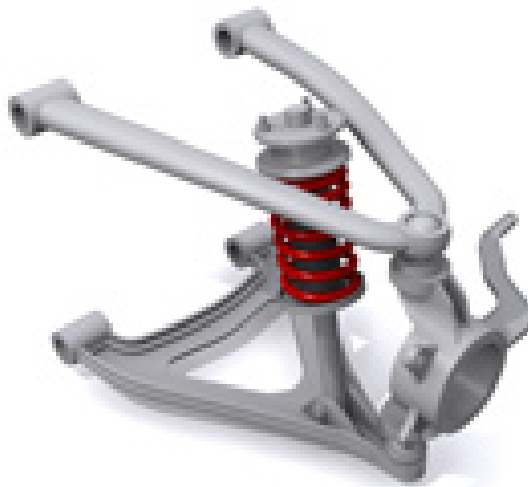
Figure 2.3: Double wishbone suspension type 1 [6].

2.2.2.3   Multi-Link Suspension

This is the latest modification of the double wishbone suspension mentioned earlier and typically for non-steering rear suspensions. The basic principle being same, each arm of the wishbone is a separate component instead of solid upper and lower wishbones. In this case, the spindle turns a small amount for steering the vehicle with jounce. It changes the geometry of the suspension due to jounce and is called "Bump Steer" [6].

Figure 2.4: Multi-link suspension [6].

This type of suspension systems find their applications in sports cars. it provides better handling, good road holding properties. A lot of variations are present in this configuration, with differences in complexities and number of joints, positioning of links, number of arms etc.

2.2.2.4   Solid-Axle Leaf-Spring Suspension

Solid-Axle Leaf-Spring suspension is a beam axle system and is generally used for heavy duty rear suspensions. It is very simple and strong. The drive axle is clamped to the leaf springs as shown in figure 2.5 using U-bolts. The dampers are directly connected between the drive axle and the chassis. The leaf springs are directly connected to the chassis through its front end point and shackles at the rear. The major drawback of this suspension is the high unsprung weight of the axle. Beam axle

suspensions are also less adjustable during wheel alignment.
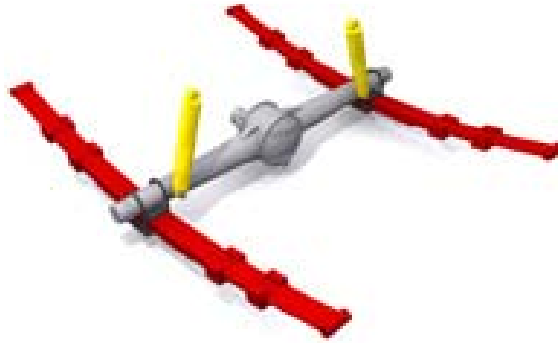
Figure 2.5: Solid-axle leaf-spring suspension [6].

2.2.2.5 Panhard Rod & Watt's Linkage

A panhard rod is a suspension link which restricts the lateral movement of the suspension. As shown in figure 2.6a, it consists of a rigid bar running sideways in the same plane as the axle, which connects one end of the axle to the car chassis on the opposite side of the vehicle. It is used along with trailing arms which stabilize the axle in longitudinal direction. Due to its excessive sideways movement between the axle and the body in short axle cars, it is not used on smaller cars. In order to overcome this problem a suspension design known as Watt's linkage is used to reduce the sideways movement [7].
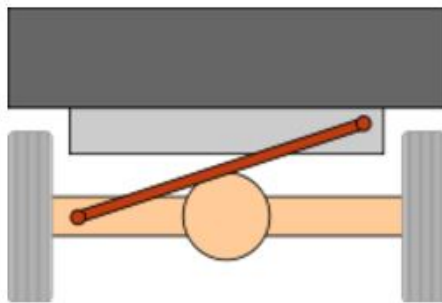
(a) Panhard rod [7].
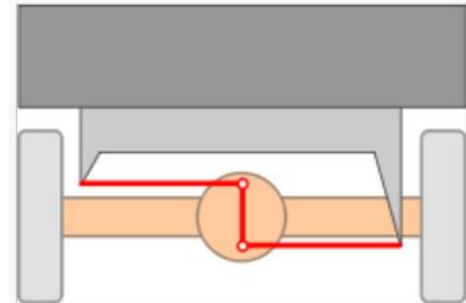
(b) Watt's linkage [8].

Figure 2.6: Rear suspension modifications.

Watt's linkage approximates a vertical straight line motion more closely than a panhard rod. It consists of two equal length horizontal rods mounted on each side of the chassis as shown in figure [8]. A short vertical bar connected between these two rods, with its center mounted to the center of the axle, is constrained in a straight line motion [8].

2.2.2.6 Air Suspension

Air suspension provides easily adjustable ride height. A good designed air suspension system can overcome metal spring suspension in any situation. Air suspension is powered by an engine driven air compressor. The air is pumped into flexible bellows, made from reinforced rubber. The air pressure inflates the bellows, and raises the chassis from the axle [9].

Figure 2.7: Air suspension of a Cadillac DeVille.

2.2.3 Suspension Wheel Alignment Angles

The position of the wheel relative to the car, the ground and each other is determined by three main wheel alignment angles. Among different suspension angles, the research is inclined to study the effects on camber, toe and caster. Camber and Toe are directly related to the wheel while Caster is a measurement of the of the suspension geometry [11].

2.2.3.1 Camber Angle

Camber angle is defined as the inclination of the tire from the vertical plane with respect to the ground when looking at the vehicle from the front view. Camber angle for most road cars vary between $0°$ to $-1.0°$ while for performance road cars it is in the range of $-1.0°$ to $-2.0°$ [11]. When the vehicle is steering, the camber angle is affected by the kingpin caster angle and kingpin inclination angle, and this therefore can influence the turn-in and handling in small-radius corners [12]. During cornering, the tires are forced to camber on both sides, this forced camber is never equal to the roll angle, but one will camber out and one will camber in [13]. Thus, during cornering the total camber angle is the addition of roll angle and camber angle obtained from the kinematics of the suspension.

Camber angle is negative when top of the tire tips inside towards the vehicle centerline as shown in figure 2.8. Cornering performance can be increased by putting some extra negative camber. However, too much negative camber can have adverse effects on tire wear, stability and ride quality.

Figure 2.8: Negative camber [14].

Camber angle is positive when top of the tire tips outside away from the vehicle centerline as shown in figure 2.9. Positive camber is used in off-road vehicles such as tractors since it helps to achieve lower steering effort. It is also used left side of

NASCAR cars to improve left turn cornering force. [15].
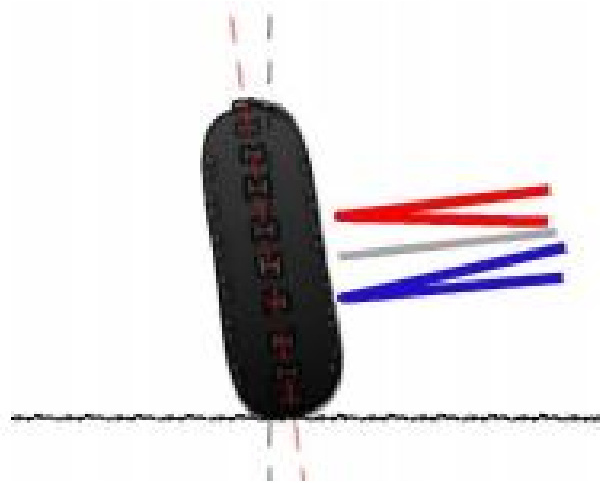
Figure 2.9: Positive camber [14].

2.2.3.2   Caster Angle

Caster is defined as the inclination of the steering axis relative to the vertical when viewed from the side of the vehicle. Steering effort and the amount of camber change during steering is effected by the amount of caster angle [16]. Caster is typically biased to the left side to compensate for road crown.
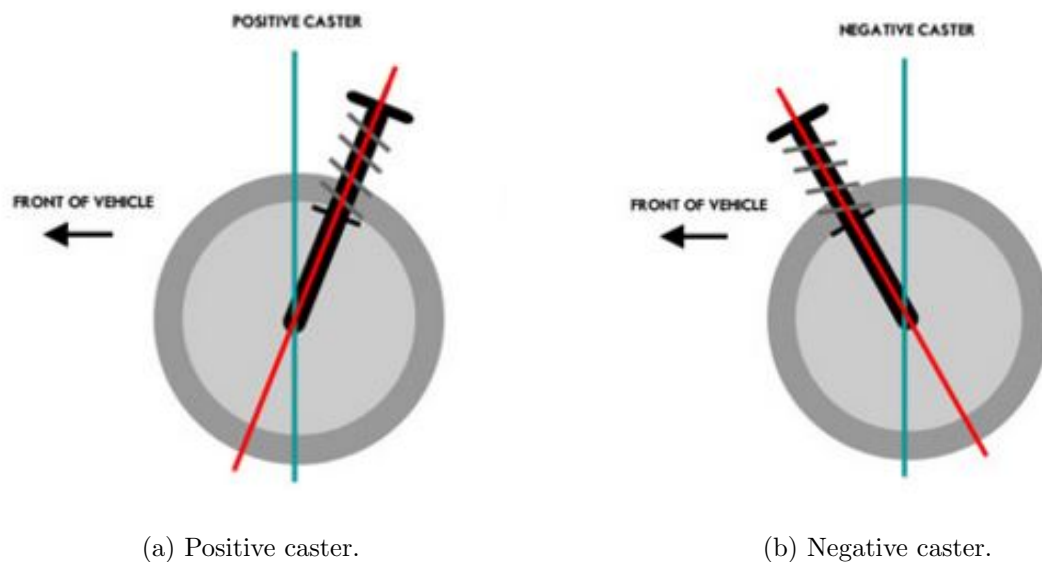
(a) Positive caster.   (b) Negative caster.

Figure 2.10: Caster angle [15].

Caster is positive when the upper pivot is behind the lower pivot as shown in figure 2.10a. Most the street cars have positive caster due to its high speed stability and improved sensitivity. It is important that the caster angle positive because it effects the aligning moment which helps to correct the steering itself when driver lets go off the steering wheel [13]. Typical range of positive caster is between $+3°$ to $+7°$ [16].

Caster is negative when the upper pivot is ahead of the lower pivot as shown in figure 2.10b. Modern vehicles do not use negative caster and would only be found on older vehicles. Negative caster has tendency to wander the car down the road but they reduce the steering effort.

2.2.3.3   Toe Angle

The wheel angle relative to the centerline of the car when viewed from the top the vehicle is referred as toe angle. Toe is generally a fraction of a whole degree and has large effects on tire wear and steering inputs. Generally a small static toe-out is given for driven wheels while a small static toe-in is given for undriven wheels in order to bring toe angles to zero in dynamic conditions [12].
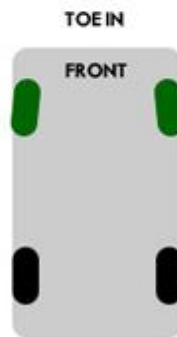
Figure 2.11: Toe-in [15].

Toe-in occurs when the leading edge of the tire points in towards the vehicle centerline as shown in figure 2.11. Static toe-in is greater in street cars than race cars to avoid the condition wherein the bushing compliance allows wheels to assume a toe-out condition [16]. Too much front toe-in affects corner turn-in, giving an

unprogressive and imprecise steering feel [12].

Toe-out occurs when the leading edge of the tire points away from the vehicle centerline as shown in figure 2.12. Toe-out improves turn-in response but also increases tire wear. Race cars generally have toe-out for sharper turn-in at the cost of stability.

Figure 2.12: Toe-out [15].

2.3   Suspension Stiffness

Vehicle stability, controllability and ride comfort are the crucial functions of a suspension system and hence it is important to study suspension compliance, compliance steer and wheel alignment variation. Suspension stiffness has an effect on the compliance, compliance steer and wheel alignment variation [17]. Orientation of the wheels and steering axis with respect to the chassis and with respect to the ground changes owing to suspension travel. The change in wheel alignment parameters due to suspension travel, the coupling in the suspension and steering systems manifests itself [18]. This change in wheel alignment parameters causes directional instability and tire wear. The optimization of the suspension design to reduce the change in wheel alignment parameters to zero is not possible with the existing architecture. Hence, the optimization of spring stiffness K is used as a solution to this problem. The solution is a compromise for comfort which demands significant suspension travel and hence a soft spring, and directional stability which requires minimal change in wheel alignment parameters and hence a stiff spring [18]. In existing designs wheel alignment

parameters are affected by suspension travel and leads to several problems. Unnecessary tire wear is caused due to changes in camber and toe during suspension travel under overload conditions. This can be a serious issue in trucks/trailers as the wheel alignment parameters can change from unloaded to fully loaded conditions. Under offset load, directional instability or pull of the vehicle can occur due to camber, caster or toe spread during suspension travel. Change in toe during suspension travel due to road undulations leads to bump steer [18]. Since the wheel alignment parameters cannot be independent of suspension travel, car manufacturers optimize the spring stiffness to get a compromise solution for comfort and control. The stiffness of the spring K is governed by the equation $K=F/X$ where F is the force applied and X is the extension or compression of the spring.

2.3.1   Soft Springs

A soft spring suspension delivers a comfortable ride on a relatively smooth road, but the passengers move up and down excessively on rough roads. The softer the springs, the more compression on outer springs and extension on the inner springs while steering the vehicle [19]. A soft spring has a low spring rate and deflects more under a given load. With soft springs, the front end dives significantly when braking. Soft springs decrease ride harshness and tires follow bumps more effectively, possibly improving traction but decreasing the rolling resistance. A spring should be soft enough to give a comfort ride, yet able to absorb all the energy from road bumps and it should be stiff enough to prevent excessive roll during steering [20]. Hence, a softer suspension will provide a comfort ride at the cost of vehicle stability and significant change in wheel alignment parameters.

2.3.2   Stiff Springs

Stiff springs are generally used in race cars due to their advantage for directional stability. Stiffer springs reduce suspension travel due to G-force loading. Increasing the stiffness increases the responsiveness to driver actions and reduces driver correction

time [21]. Increasing the stiffness, increases harshness causing reduced traction. The wheel assembly is fixed at some point and travels up and down in an arc instead of a linear path. When the vehicle hits a bump, the wheel travels and the body stays put or vice versa, it impacts the camber angle which changes the tire contact patch [22]. Limiting the wheel travel can reduce the camber change improving stability and performance. Stiff springs can reduce wheel travel and hence produce minimal changes in wheel alignment parameters.

2.4   Suspension Bushings

A bushing can also be a vibration isolator providing not only an interface between two parts but also damping the energy transmitted through the bushing. A bushing allows certain movement while separating the faces of two metal objects [23]. Though it reduces vibrations in the chassis from the ground, the flexibility introduces an element of play in the suspension system. This play results in a change in wheel alignment parameters such as camber, caster and toe during cornering and braking, affecting the vehicle's handling. Hence, bushings made of high stiffness materials such as polyurethane are used as replacements for rubber suspension bushings. Figure 2.13 shows typical rubber and aftermarket polyurethane bushings used on cars.

Figure 2.13: Rubber bushing (left) and Polyurethane bushing (right) [24].

When the vehicle accelerates, brakes, turns or cruises, the rubber bushings in the suspension system have compliance and deflect slightly changing the wheel alignment. Rubber bushings provide a soft ride but over a time, rubber begins to wear and the

suspension components may start to bind. Rubber is a softer (less stiff) material than polyurethane, and hence dampens the noise and vibrations entering the chassis. The bushings stretch and compress as the suspension travels and the rubber begins to wear and distort causing the suspension to work less efficiently [24]. Worn out bushings one one the major reasons for mis-alignment. Rubber bushings are chemically bonded with the metal shell and hence no squeaking occurs as it is affixed to the metal. Since they are bonded with metal shell there is no need to grease them. All the benefits mentioned above would be advantages if we never cornered the car. As the rubber stretches and compresses, it changes the suspension alignment and affects handling. Figure 2.14 shows deformation of a rubber suspension bushing when car enters a turn.
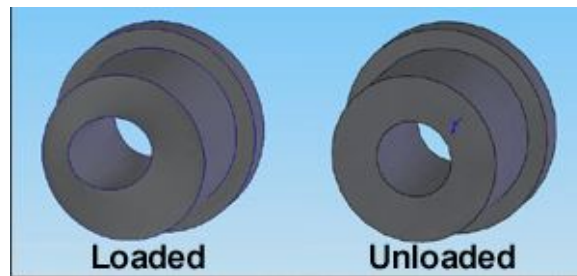
Figure 2.14: Deformation of bushing in loaded condition [25].

As seen from figure 2.14 the hole center moves to one side under loaded conditions. This causes a camber loss on front suspension while turning. This change in camber change causes loss if traction while turning. Figure 2.15 shows how the rubber bushings affects camber angle which lifts the contact patch and reduces traction [25].

The problems of change in wheel alignment parameters can be overcome by the use of polyurethane bushings. Polyurethane bushings are extremely rigid and much stiffer that they do not flex like rubber bushings. Since they are stiff more noise and vibrations will be transferred to the chassis [24]. These bushings last a lifetime as the material is resistant to wear, heat , oils and other road chemicals. Since these bushings are not chemically bonded with metal they can squeak if not greased properly. Suspension bushings are subject to flexing in multiple planes and also applied torque
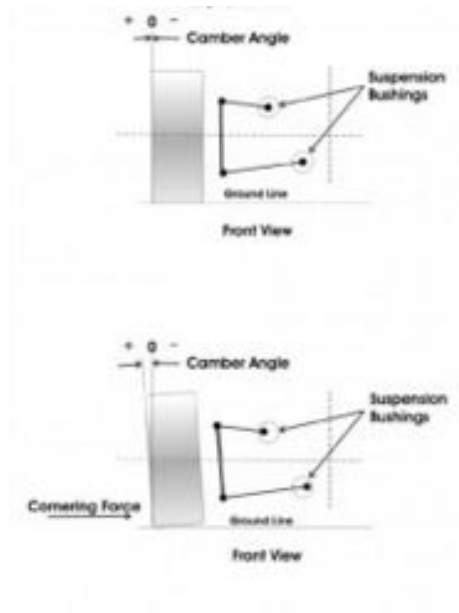
Figure 2.15: Camber shift due to deformed bushing [25].

of A-arm as it rotates on th cross shaft [25]. Figure 2.16 shows the magnitude of flexing in a rubber bushing over polyurethane bushing under similar load conditions.
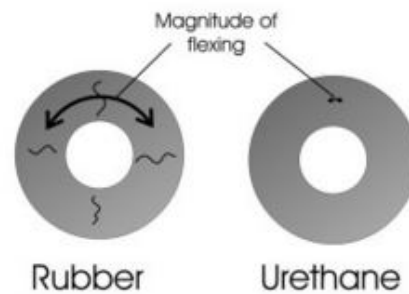
Figure 2.16: Magnitude of flexing in Rubber and Polyurethane bushings [25].

Rubber and polyurethane, different in comfort and handling, are actually more on the middle ground in the diversity of bushing material. To sum it up, rubber bushings provide a comfort ride at the cost of vehicle handling due to change in wheel alignment parameters while polyurethane bushings provide excellent vehicle handling with minimal change in wheel alignment parameters at the cost of ride quality.

2.5   Types of Wheel Alignment

Wheel alignment depends on the suspension design and not all vehicles are easily adjustable or fully adjustable. Some vehicles require aftermarket adjustment kits to allow sufficient adjustment to compensate for vehicle damage or the change in alignment by the use of other aftermarket performance kits. The different types of alignment known today are front-end alignment, thrust angle alignment and four-wheel alignment which are explained in the following sections.

2.5.1   Front-End Alignment

As the name suggests, front-end alignments only measures and adjusts front axle angles. It is the simplest and basic alignment method. Front-end alignments are good for some vehicles with a solid rear axle. Even though front axle angles are aligned it is important to check that the front tires are positioned correctly in front of the rear tires. Front-end alignment is not sufficient on most of the modern cars and considered as obsolete due to its incomplete nature [26].

2.5.2   Thrust Angle Alignment

This alignment goes a step further by conducting a thrust angle alignment and includes front-end alignment explained above. A thrust angle alignment is performed to confirm that all four tires are "square" with each other. To get better results on road in terms of tire wear and safety, a thrust alignment is a must for all vehicles with a solid rear suspension. Vehicles that can "dog track" going down the road with the rear offset from the front can be identified through thrust angle alignments [26].

The imaginary line drawn perpendicular to the rear axle's centerline defines the thrust angle as shown in figure 2.17. It indicates whether the rear axle is lined up the centerline of the vehicle. It also tells if the rear axle is parallel to front axle and ensures that the wheelbase is same on both sides of the vehicle [26]. An out-of-position axle or incorrect toe settings can result in incorrect thrust angles. Incorrect thrust angles cuase the vehicle to handle differently when turning left vs. turning right [26].
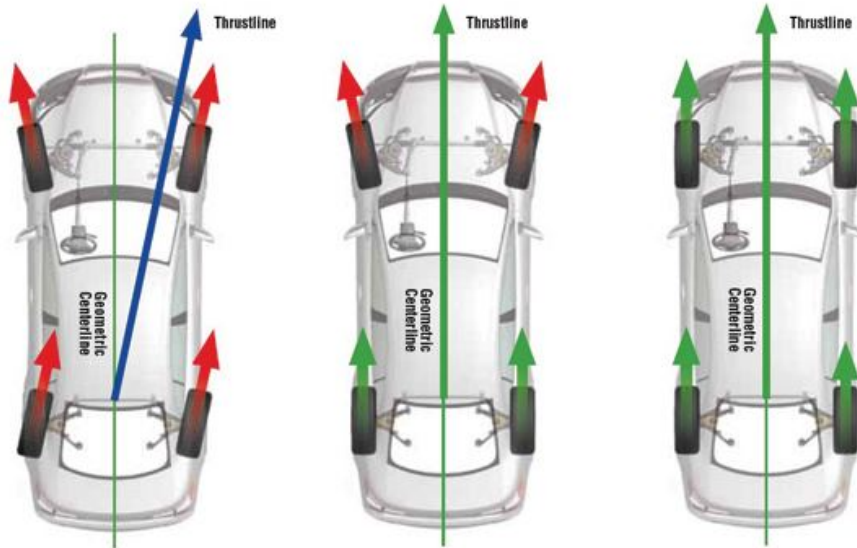
Figure 2.17: Thrust angle [27].

If the thrust angle is incorrect on a vehicle with solid rear axle, it might be necessary to straighten the frame and position the rear axle correctly.

2.5.3 Four-Wheel Alignment

Vehicles with four-wheel independent suspensions or front-wheel drive vehicles with adjustable rear suspension are recommended to undergo a four-wheel alignment. This alignment requires more man power as the procedure measure and adjusts rear axle angles in addition to front axle angles. Four-wheel alignment is the most common type of alignment performed today [26]. This alignment goes one step further by measuring and adjusting the rear axle angles, which is a combination of front-end and thrust angle alignments. All four corners are restored to manufacturer's specifications in this alignment method [27]. Being the most comprehensive alignment, it demands special equipment and skilled labor.

2.5.4 Mechanical v/s Computerized Wheel Alignment

Wheel alignment can be carried out in many different ways using measurement principles from a straight aluminum bar to the modern touch-less systems. The method adopted depends upon the application and the accuracy required for mea-

surements. A brief description of the methods used for wheel alignment is given in the following sections.

2.5.4.1 Mechanical Wheel Alignment

Mechanical wheel alignment can be performed in different ways by the use of strings, angle gauge, aluminum bars, turn plates, etc. This trivial method is mostly used by race teams because of its accuracy and repeatability. Since the modern computerized systems are not well equipped for aligning race cars, the mechanical measurement method comes handy.

Toe measurements can be done with a straight aluminum bar, amongst the measurements for wheel alignment. With a straight aluminum bar and a sufficient knowledge about alignment, one can adjust toe with an outcome superseding to that of wheel-clamp based aligners. The benefit from the use of aluminum bar is the fact that small angles give more deviation along longer distances [28].

The toe measurements by aluminum bar are now replaced commonly using strings also known as 'String Method'. The string method gives accurate toe measurements and can be done simultaneously on all four wheels with proper equipment. Along with simultaneous alignment it ensures that all the wheels are square so that the rear axle runs true and parallel to the front axle. The strings are attached to the car as shown in figure 2.18 and move with the car, hence, the car can be rolled to settle the settings after the adjustments are made without affecting the measurements [29].

Figure 2.18: Toe alignment using strings [29].

The string bars are positioned such that the distance from the tires to the bars is equal from side to side. Also it should be ensured that the front and rear string bars are adjusted so that the distance from the center of the wheel to the string is equal side to side as shown in figure 2.19.
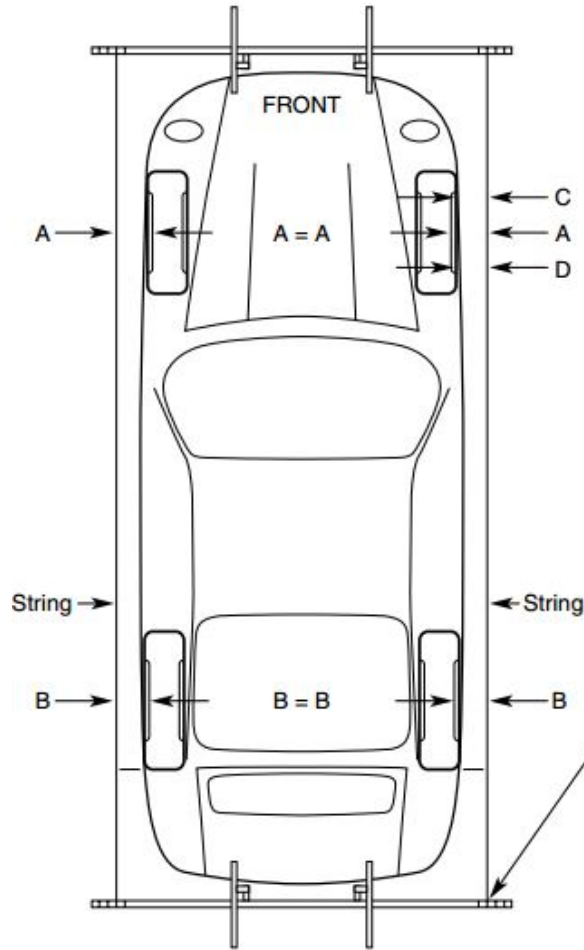
Figure 2.19: Toe alignment setup layout [29].

The measurements can be noted down using a steel rule or tape measure with the decimal scale upto 1/32" on one side and metric on the other, roughly 12" long. The toe measurement requires two measurements per wheel, one on the leading edge and one on the trailing edge. Measure the leading edge of the wheel first and then measure the trailing edge, compare the measurements and determine the toe using the graph shown in figure 2.20. The operator must be consistent while taking measurements to

get accurate toe readings [29].
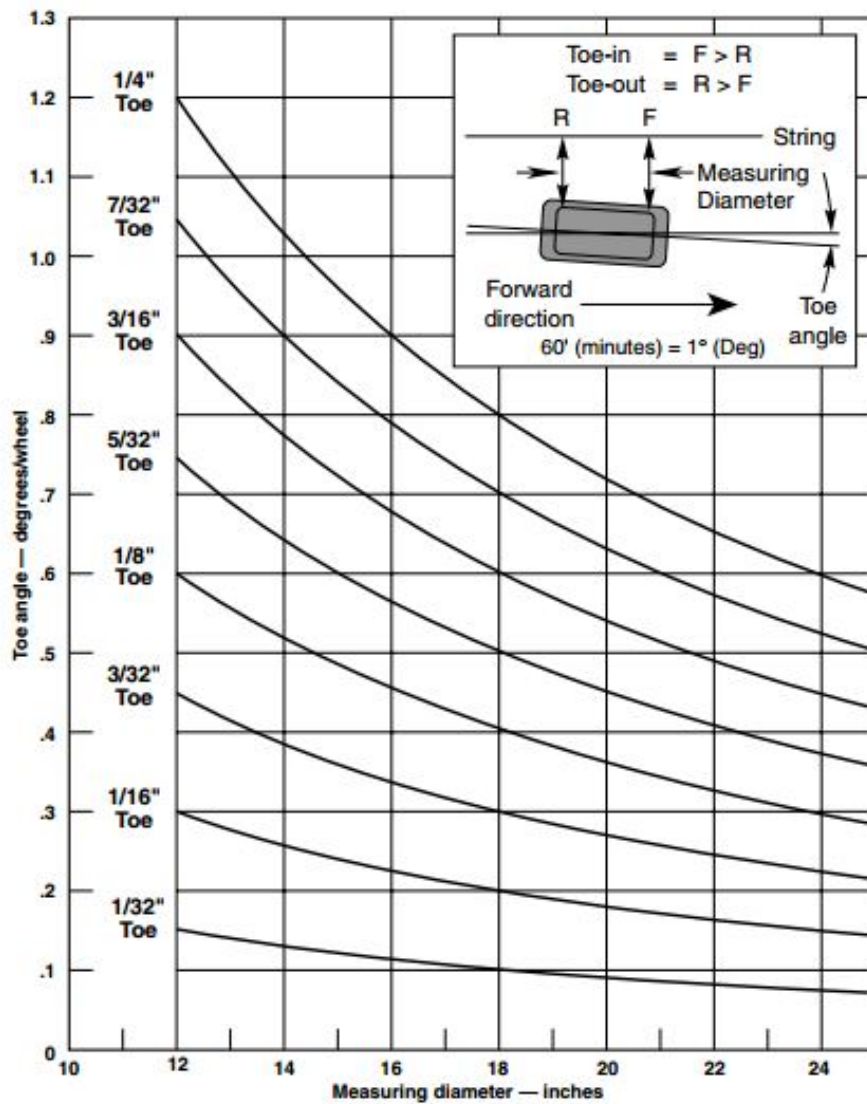
Figure 2.20: Toe settings at various tire diameters per wheel [29].

For toe-in, measurement is longer on the leading edge of the wheel than the trailing edge of the wheel. As per the layout shown in figure 2.19 measurement C will be longer than measurement D for toe-in. For toe-out, measurement is shorter on the leading edge of the wheel then the trailing edge of the wheel. As per the layout shown in figure 2.19 measurement C is shorter than measurement D [29]. The toe angle can interpolated from the graph in figure 2.20 for the measured wheel diameter and desired

toe angle. It is important to note that the toe angle in degrees remains unchanged with diameter but changes with decimal settings.

The first approaches for measuring camber used a pendulum which intersected a scale marked in degrees as shown in figure 2.21. The principle of the measurement is to use earth's gravity as a reference that is available everywhere.
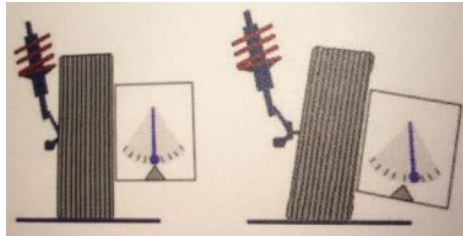
Figure 2.21: Schematic of camber measurement using pendulum [28].

With the advancement in technology, camber measurement became more easy. With the availability of digital inclinometers camber was measurable electronically, and more important computer based. Now there are digital gauges which are programmed to give camber and caster reading in a matter of seconds. The gauge after calibrating with respect to the ground surface can be simply attached to the wheel at three points using clamps and the measurement of the desired angle is displayed on the screen as shown in figure 2.22.

Figure 2.22: Camber measurement using camber/caster Gauge [29].

2.5.4.2 Computerized Wheel Alignment

Computerized alignment systems use lasers or infrared sensors for measurements. The readings for camber, caster, toe and thrust angle are displayed on a computer screen. The machine is equipped with built in calibration system and can be calibrated by the operator. The computerized wheel alignment machine operation can be divided into two basic principles, internally referenced measurement systems and externally referenced measurement systems [28]. Internally referenced measurement systems have all the components mounted on the car, e.g. sensor heads which are used in this research as shown in figure 2.23a. Externally referenced measurements systems have the laser targets mounted on the wheel while the laser sources are mounted away from the car on a separate stand as shown in 2.23b.

(a) Internally referenced measurement systems.

(b) Externally referenced measurement systems.

Figure 2.23: Computerized wheel alignment systems [30].

The difference between the two systems is that in externally referenced measurement systems, the reading of the sensors change as the car moves. As a result, the system has to determine the position of the car permanently and take that into consideration while giving out true toe and camber values [28]. In the case of internally referenced systems, the toe readings stay the same more or less even if the car is pushed on the turn plates, given that the steering angle is same [28]. The internally referenced systems evaluates atleast 6 different measurement distances. These systems

first measure the position of the wheel centers in interference to each other using the six different simultaneously measured angles as shown in figure 2.24 [28].
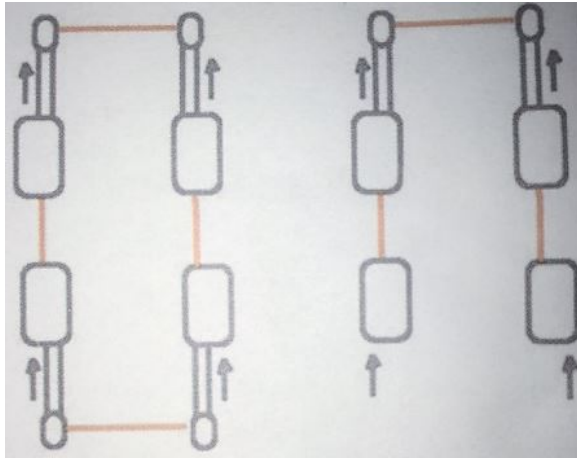
Figure 2.24: 8-sensor system (left), 6-sensor system (right)[28].

After getting the position of each wheel center, the respective angles of the wheels are determined with respect to the wheel center. As shown in figure 2.24 one red line represents two laser beams in opposite directions but not coincident, and a minimum of six measurement lines are required four transversal and two lateral to measure four individual toe values [28]. Most of the alignment machines nowadays use full 8-sensor measurement system as shown in figure 2.24. This enables coarse toe measurement required for higher steering angles, when front transversal toe sensors no longer interact with each other. The caster sweeps of 20° can be done without angle sensors on turn tables with 8-sensor system [28].

Internally referenced measurement systems do not have the knowledge about actual distances but only angles. They estimate the distances by using measured angles and reference distances from the data taken from sensor heads. On the other hand, externally referenced measurement systems know the car dimensions from the measurements taken. Externally referenced systems have an external set of cameras which are not connected to the car, and easy-to-recognize pattern printed targets clamped on the wheels. The principle of measurement lies in the fact, that a certain shape,

e.g. circle, will look bigger or smaller, depending on the distance from the camera lens, and the same circle will look like an oval from a different angle. The software uses this image from the camera lens to analyze the deformations and gives out the results. The quality of the results also depend on the mounting of the clamps carrying the pattern printed targets [28].

2.6 Working of Vehicle Alignment Sensor System

The alignment machine used for this research consists of a conventional head sensor system, DSP700 series, from Hunter Engineering Company as shown in figure 2.25 which uses optical sensors for wheel alignment measurements. A brief description of the working principle of the optical sensors is given in the following sections.

Figure 2.25: DSP700 series conventional head sensor system[30].

The vehicle alignment sensor system consists of pairs of sensors acting as active and passive sensors, cooperating with each other in order to determine the wheel alignment angles. It includes a first sensor assembly which measures at least first angle with respect to a fixed reference which is related in predetermined manner to an angle of the vehicle to be aligned. A second sensor assembly being mounted on the other wheel and having a geometrical relationship with the wheel of the vehicle being aligned. The first sensor consists of at least one detector and the second sensor has at least a pair of emitters which are in fixed geometrical relationship with each other. The relative alignment angle of the vehicle is determined by using the detector which measures the apparent geometrical relationship of the pair of emitters. The true alignment angle can be determined from the first angle and the relative alignment

angle. Calibration of the sensor system is also performed by using the first and second sensor assembly [31].

2.6.1 Measurement of Angles

Computerized wheel alignment systems make use of optical sensors at each wheel and the geometrical relationship between the sensors is used to calculate the wheel alignment angles. The following sections describe the toe and camber angle measurements using sensors and the calibration method involved for taking accurate measurements.

2.6.1.1 Brief Summary of the Working Principle

The vehicle alignment sensor system includes a first sensor assembly and a second sensor assembly to be mounted on the wheel of the vehicle to be aligned in a known geometrical relationship. The first sensor assembly has one detector and the second sensor assembly has a pair of emitters in a fixed geometrical relationship. The toe alignment is determined by the detector which measures the apparent geometrical relationship with the pair of emitters [32].

In the second aspect of the working principle, the first sensor assembly has a detector and the second sensor assembly has a pair of emitters which are mounted on the wheel and have fixed geometrical relationship. The camber angle is determined by the detector which measures the apparent geometrical relationship with pair of emitters [32].

In the third aspect, first camber angle is measured at the first wheel with respect to a fixed reference, with a second sensor assembly with a pair of emitters mounted on the second wheel in a fixed geometrical relationship with each other. The detector measures the apparent geometrical relationship with the pair of emitters determining the relative camber angle of the second wheel. The true camber angle of the second wheel is determined from the measured first camber angle and the relative camber angle [32].

In the fourth aspect, the apparatus is calibrated for determining camber angles by disposing all the sensor assembly in a fixed geometric relationship with the wheels of the vehicle to be aligned. Each sensor assembly has a gravity referenced inclinometer to determine the camber angle of the wheel. Each sensor assembly has a fixed geometrical relationship with at least one of the wheels having a pair of emitters at a known orientation and determines the relative camber angle of that wheel along with the true camber angle. By comparing the true camber angle of the second wheel derived from the pair of emitters and the camber angle of the corresponding wheel obtained from the corresponding gravity referenced inclinometer, the calibration of the corresponding sensor assemblies can be determined [32].

In the fifth aspect, at least first and second sensor assemblies are disposed in a fixed geometrical relationship with the corresponding wheels of the vehicle. Each sensor assembly has a detector and a pair of emitters for determining the true toe angles of the wheels. The toe angle is determined from the detector and emitter pair by disposing a fixed geometrical relationship with at least one of the wheels of a vehicle. A second toe angle of the wheel is determined using a pair of emitters by disposing a fixed geometrical relationship with another wheel of the vehicle. The calibration of the toe angle measurements is checked by comparing the first toe angle to the second toe angle [32].

2.6.1.2   Description of the Embodiment

Figure 2.26 is a diagrammatic view of the wheels of the vehicle, with the wheels intentionally misaligned for illustrating the wheel alignment geometry. The instruments along with measured angles and geometry lines are referenced with numbers and alphabets in the figure 2.26. The alignment calculations are done with respect to the geometry line 30. The line of sight T between the instruments 21L and 21R is the optical beam path from the respective instruments. The line of sight L between instruments 23L and 24L, and the line of sight R between the instruments 23R and
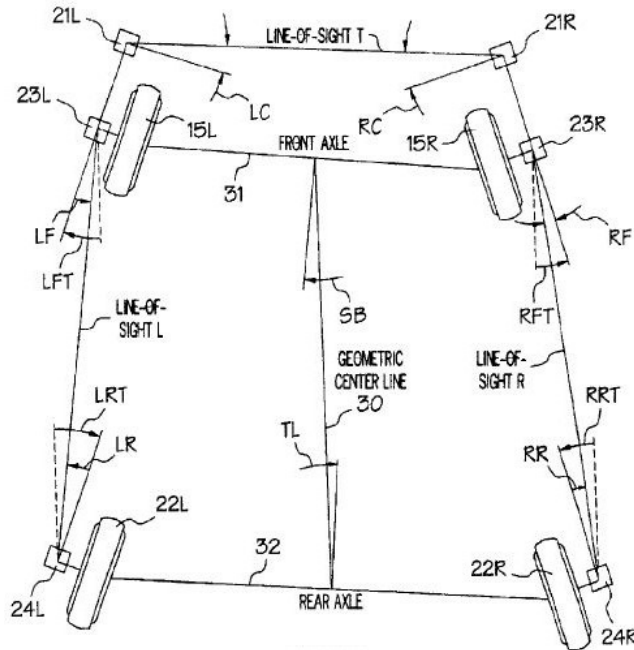
Figure 2.26: Diagrammatic layout of the vehicle [32].

24R represents the optical beam path from those instruments. The construction lines parallel to th e geometric center line 30 acts as a reference fro the angles [32].

The angles pertinent to the alignment determination as shown in figure 2.26 are computed relative to the geometric centerline 30 as shown in table 2.1:

Table 2.1: Algorithm of computation of toe angles [32].

Angles Computated	Algorithm
LFT (left front toe)	$\frac{1}{2}$(LC + RC + LF - RF)
RFT (right front toe)	$\frac{1}{2}$(LC + RC - LF + RF)
TFT (total front toe)	LFT + RFT = LC + RC
SB (setback)	$\frac{1}{2}$(RC - LC + LF - RF)
LRT (left rear toe)	LFT - LF + LR = (LC + RC - LF - RF) + LR
RRT (right rear toe)	RFT - RF + RR = $\frac{1}{2}$(LC + RC -LF - RF) + RR
TRT (total rear toe)	LRT + RRT = LC + RC - LF - RF + LR + RR
TL (thrustline)	$\frac{1}{2}$(LRT - RRT) = $\frac{1}{2}$(LR - RR)
LFTTH (left front toe relative to thrust line)	LFT - TL
RFTTH (right front toe relative to thrust line)	RFT - TL

Figure 2.27 shows a pair of emitter A-A placed along line 217 and emitter B located behind line 217 separated by a distance referred as 218. The figure depicts the top view of the wheel along the Z-axis. The emitter pair A-A is separated by a distance referred as 219. The emitter B is behind the midpoint of the emitter pair A-A parallel to X-axis [32].
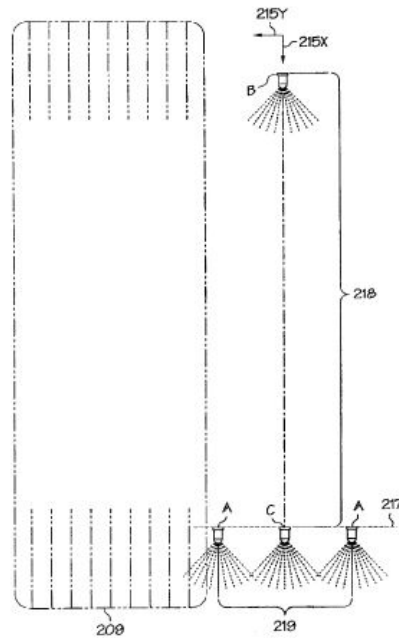
Figure 2.27: Schematic top view of emitter configuration [32].

Figure 2.28a and figure 2.28b show the geometric relationship of the emitters with respect to the detector. The detector has line of sight 232 to emitter B and line of sight 234 and 236 to emitter pair A-A. Figure 2.28b as viewed from the front, the apparent horizontal distance between left emitter A and emitter B is d1 and equal to d2 which is the horizontal distance between right emitter A and B. The horizontal separation between emitter pair A-A is d3. Each of these horizontal distances are identified by the detector placed on the front sensor [32].

Figure 2.29a and 2.29b show the positions of emitter A-A, B and C for two different toe orientations of the wheel as observed from the front of the vehicle. Apparent distances between emitters are marked as d1'-d3' and d1''-d3''. Depending on the
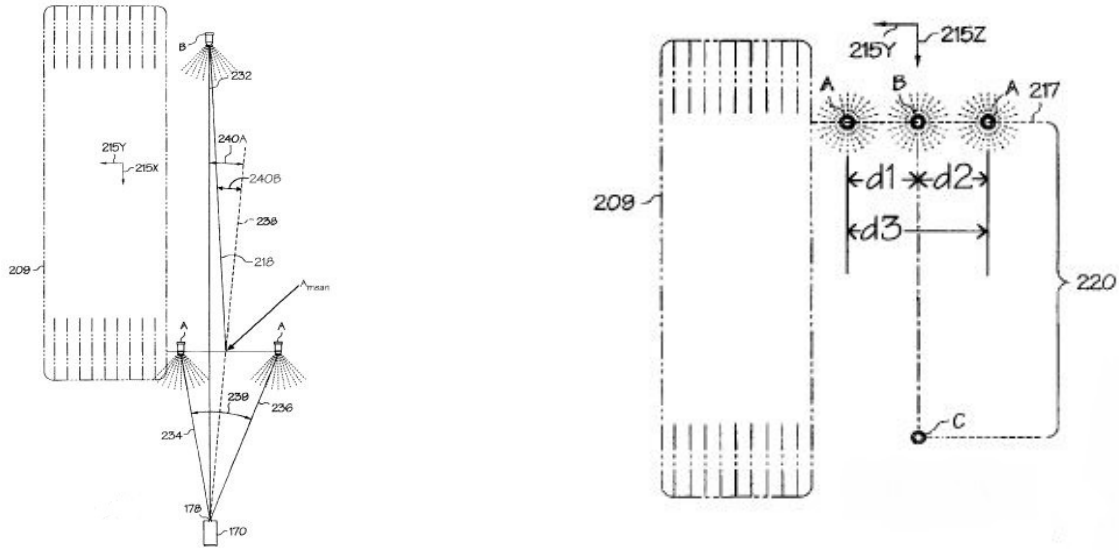
(a) Schematic top view showing sensor line of sight for toe.

(b) Schemmatic front view showing sensor line of sight for toe.

Figure 2.28: Front and top view of sensor placement [32].

observation angle each of the apparent distances change in a mathematical relation with the observed angle. The ratio of apparent distance d1 and d2 to d3 changes in proportion to the observed angle 240A. Using the observed apparent distances and actual horizontal distances between the emitters, the observation angle 240A can be computed using trigonometric relations.

(a) Front view of wheel with small toe angle.

(b) Front view of wheel with large toe. angle

Figure 2.29: Apparent displacement of emitters at different longitudinal toe angles [32].

Determining the angle 240A as shown in figure 2.28a and measuring the distance between detector and emitter pair A-A along with known geometrical relationship between emitter pair A-A and B, angle 240B can be calculated. Referring to figure 2.28a, the distance from emitter B to the midpoint of emitter pair A-A i.e. A_{mean} is denoted as D_1. The distance from aperture 178 to A_{mean} is denoted as D_2, which determined electronically. Using the Law of Sines, angle 240B can be calculated as follows [32]:

$$240_B = 240_A + \sin^{-1}\left(\frac{D_2}{D_1}\sin(240_A)\right) \tag{2.1}$$

Angle 240B refers to the longitudinal toe of the rear wheel with respect to line of sight 238 from the front wheel as shown in figure 2.28a. In a similar manner, transverse toe values can be determined and hence total four wheel toe alignment can be determined.
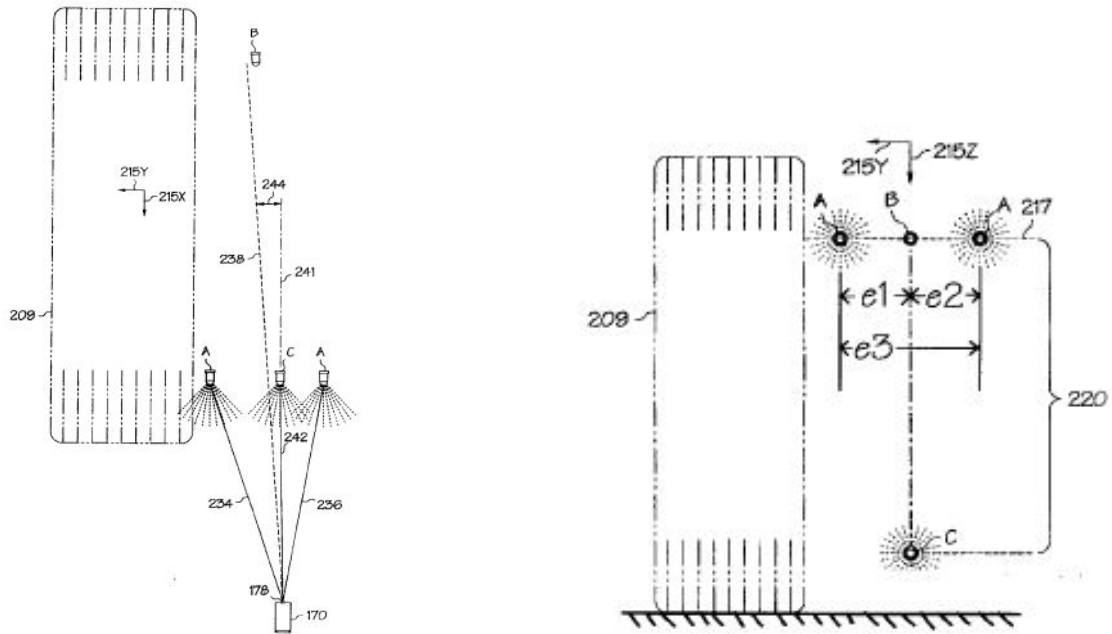
(a) Schematic top view showing sensor line of sight for camber.

(b) Schematic front view showing sensor line of sight for camber.

Figure 2.30: Front and top view of sensor placement [32].

The discussion is not only limited to determination of toe angles but also allows measurement of relative camber between two adjacent sensor assemblies. The geometric relationship shown in figure 2.30a and 2.30b is used to measure the relative camber between two adjacent sensor assemblies. Even though the sensor assemblies can only measure angles in its horizontal planes, the relative horizontal positions of emitters A-A and C can be used to measure camber of the rear wheel relative to the front assembly [32].

(a) Front view of wheel with small camber angle.

(b) Front view of wheel with large camber angle.
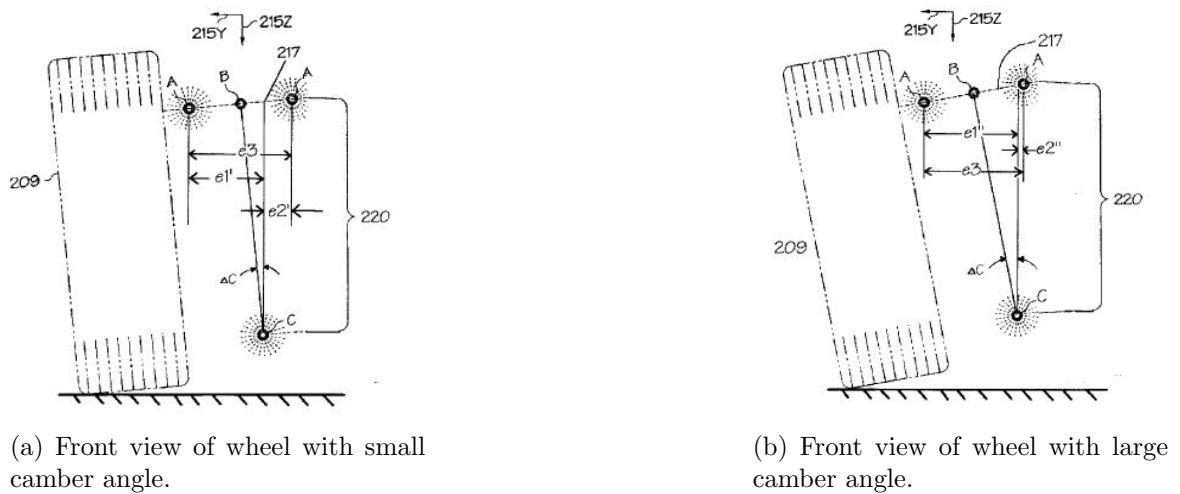
Figure 2.31: Apparent displacement of emitters at different camber angles [32].

Referring to figures 2.30b, 2.31a and 2.31b, the apparent horizontal distance between left emitter A and emitter C is denoted by e1, e1' and e1'' respectively, while that of right emitter A and emitter C is denoted by e2, e2' and e2''. The apparent horizontal distances e1, e2 and apparent emitters A-A separation e3 is determined by the detector disposed on the sensor assembly. The distance between emitters A-A denoted by e3 is referenced as 217 and the vertical separation with emitter C is referenced as 220 as shown in figure 2.30b. The detector measures the angle subtended by distance e1, referred as 244B, and angle subtended by e3, referred as 244C as seen from the observation angle. For small angle measurements, the ratio of 244C to 244B can be approximated by ratio of e3 to e1. Using trigonometric relations, the relative

camber angle, ΔC can be expressed as [32]:

$$\Delta C = \sin^{-1}\left(\frac{e1 - \frac{e3}{2}}{(220)}\right) = \sin^{-1}\left(\frac{e3\left(\frac{(244B)}{(244C)}\right) - \frac{e3}{2}}{(220)}\right) \tag{2.2}$$

The measured relative camber ΔC can be compared to the camber angle of the front wheel which is measured by gravity referenced camber transducer and hence the true camber value of the rear wheels can be determined [32].

The above described system of sensors can be used in coordination with conventional angle transducers to get redundant calibration measurements. The above described system has a passive array of emitters along with traditional means of measuring toe and camber. The calibration of the total four sensor system can be determined by comparing the traditional measurements and active/passive measurements. Not only the calibration is determined but also which sensor assembly is out of calibration can be detected. These calibration checks can determine both toe and camber calibration. These redundant measurements can result in more fault tolerant systems [32].

2.6.2 Wheel Alignment Sensor Runout Compensation

The runout between the sensor head and the rotational axis of the wheel on which the sensor head is clamped in each of two orthogonally related planes is measured using the measurement of the angle between the axis of rotation of the wheel and the axis on which angle sensors are supported at two or more rotational positions of the wheel, and the measurement of the rotational angle of the wheel at each rotational positions. Using these measurements a runout equation is derived which is used to compute the runout at every rotational positions of the whee [34].

The vehicle alignment sensors clamped on individual vehicle wheels must be compensated for any runout between wheel alignment sensor plane and the plane perpendicular to the wheel rotational axis. The runout compensation is obtained by rotating

the wheel and the mounting shaft to three distinct rotational positions relative to sensor housing for e.g. 120° interval as in the Mercedes-Benz logo. A sinusoidal pattern representing the amount of runout can be computed using the sensor readings for any rotational position of the wheel and sensor [35].

2.6.2.1   Brief Summary of the Working Principle

Runout measurements are carried out in single or each of two perpendicular planes at three rotational positions of wheel to which two mutually perpendicular angle sensors and position encoder are mounted. The amplitude of the runout and wheel rotational position is measured in orthogonally related planes. The recorded measurements are subsequently used to compensate wheel alignment parameters measured in two planes at any rotational position of the wheel [34].

Figure 2.32 is a schematic showing the wheel alignment sensor head mounted on the right front wheel using wheel clamps. The head carries first angle sensor referred as 16 which provides output for the angular position of the sensor with respect to the vertical plane while, the second angle sensor 18 provides output for the angular position of the sensor with respect to the horizontal plane [34].
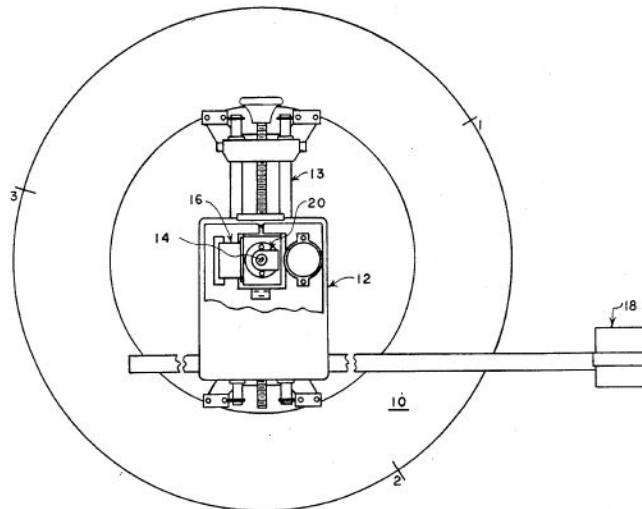
Figure 2.32: Schematic side view of sensor head mounted on right front wheel [34].

The sensor head carries an encoder referred as 20, which develops a signal during

wheel rotation. The signal developed comprises of unidirectional pulses generated for each predetermined wheel rotation. These signals are used to correlate the measurements from angle sensors 16 and 18 with the wheel rotational position. Due to wheel wobble, the actual toe and camber measurements are corrected to compensate runout [34].

The angle formed between the wheel rotation axis and the rotation axis of sensor 12, causes the sensor axis to generate a runout circle of radius R as shown in figure 2.33.
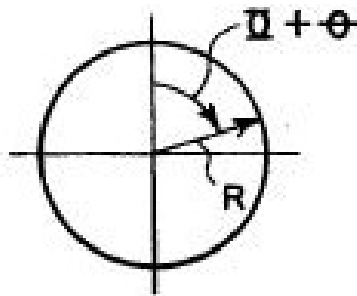
Figure 2.33: Runout circle between wheel and sensor [34].

Figure 2.34 shows the waveform of the runout circle with respect to the vertical plane. The value of camber is plotted on Y-axis and the rotational position of the wheel is plotted on the X-axis.
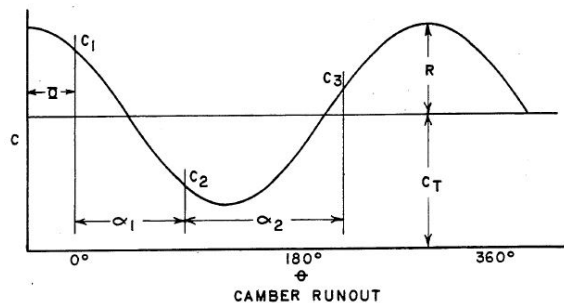
Figure 2.34: Waveform of runout in camber plane [34].

Figure 2.35 shows the waveform of the runout circle with respect to the horizontal plane. The value of toe is plotted on Y-axis and the rotational position of the wheel is

plotted on the X-axis. Camber and toe waveforms are out of phase by 90° with each other.
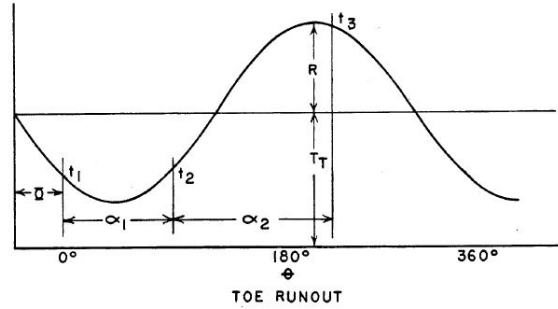
Figure 2.35: Waveform of runout in toe plane [34].

The camber runout equation is developed by rotating the wheel in clockwise direction from arbitrary from angular position 1 at which the angle of the sensor relative to vertical plane measured by angle sensor 16 and recorded by the computer to a angular position 2 and then angular position 3. The rotational position of the wheel is also recorded at each angular positions 1, 2 and 3. The variables related to figure 2.34 are as follows [34]:

θ is the angle through which the wheel is rotated relative to position 1, with clockwise being positive.

c is the camber angle as a function of wheel rotation angle.

R is the runout magnitude.

ϕ is the angle from position 1 to reference point on waveform.

C_T is the angle between position 1 and position 2.

α_1 is the angle between position 1 and position 2.

α_2 is the angle between position 2 and position 3.

The equation of the waveform is:

$$c = C_T + R \cdot \cos\left(\theta + \phi\right) \qquad (2.3)$$

The equation of the three data points are [34]:

$$c_1 = C_T + R \cdot \cos(\phi) \tag{2.4}$$

$$c_2 = C_T + R \cdot \cos[\phi + \alpha_1] \tag{2.5}$$

$$c_3 = C_T + R \cdot \cos[\phi + \alpha_1 + \alpha_2] \tag{2.6}$$

Expanding the equations 2.5 and 2.6 by substituting

$$k_{c1} = \cos[\alpha_1]$$

$$k_{s1} = \sin[\alpha_1]$$

Therefore,

$$c_2 = C_T + R \cdot K_{c1} \cdot \cos(\phi) - R \cdot K_{s1} \cdot \sin(\phi) \tag{2.7}$$

$$c_3 = C_T + R \cdot K_{c2} \cdot \cos(\phi) - R \cdot K_{s2} \cdot \sin(\phi) \tag{2.8}$$

Solving for $\sin(\phi)$ and $\cos(\phi)$ in equations 2.4, 2.7 and 2.8 and letting

$$k = k_{s1} \cdot [1 - k_{c2}] - k_{s2} \cdot [1 - k_{c1}]$$

$$\sin(\phi) = \frac{[c_1 - c_2] \cdot [1 - k_{c2}] - [c_1 - c_3] \cdot [1 - k_{c1}]}{R \cdot k}$$

$$\cos(\phi) = \frac{[c_1 - c_3] \cdot [k + k_{s2} \cdot [1 - k_{c1}]]}{R \cdot k \cdot [1 - k_{c2}]} - \frac{[c_1 - c_2] \cdot [1 - k_{c2}] \cdot k_{s2}}{R \cdot k \cdot [1 - k_{c2}]}$$

Let

$$x = \frac{[c_1 - c_3] \cdot [k + k_{s2} \cdot [1 - k_{c1}]]}{k \cdot [1 - k_{c2}]} - \frac{[c_1 - c_2] \cdot [1 - k_{c2}] \cdot k_{s2}}{k \cdot [1 - k_{c2}]}$$

and

$$y = \frac{[c_1 - c_2] \cdot [1 - k_{c2}] - [c_1 - c_3] \cdot [1 - k_{c1}]}{k}$$

Now $\sin(\phi)$ and $\cos(\phi)$ can be expressed as:

$$\sin(\phi) = \frac{y}{R}$$

$$\cos(\phi) = \frac{x}{R}$$

From basic trigonometric relations following can be deduced:

$$R = \sqrt{x^2 + y^2}$$

$$\phi = \arctan\left[\frac{y}{x}\right]$$

The equation for runout compensation as a function of wheel angle can be written as:

$$rc_\theta = R \cdot \cos(\theta + \phi) \tag{2.9}$$

Thus knowing R and ϕ, the runout correction can be specified for any wheel angle θ. Shifting the cosine function in equation 2.9 by 90°, the runout equation for toe can be written as:

$$rt_\theta = R \cdot \cos(\theta + \phi + 90°) = -R \cdot \sin(\theta + \phi) \tag{2.10}$$

Providing these runout magnitudes for camber and toe to the computer, the runout between the sensor heads and vehicle wheels can be compensated.

CHAPTER 3:   METHODOLOGY

The aim of this research is to study the influence of variables on wheel alignment measurements. This research effort include hundreds of passenger vehicle wheel alignment measurements based on their suspension types and the class of the vehicle. The design of experiments works to capture the various influential factors. A conventional alignment sensor system, Hunter Pro-Align with DSP700 wheel sensors, was used to take measurements. Accuracy of the equipment is not a big part of this study, since the equipment seems to measure to the $0.01°$ resolution which it claims. The influence of the variables on the measurements due to the suspension types and class of the vehicle encouraged me and backed my research. A consistent test protocol was followed during each measurement to eliminate undesired errors and to provide accurate data suggesting the influence of variables based on test vehicles and conditions, which is briefly described in section 3.1. A bushing stiffness tensile test was performed to see the influence of suspension bushings on vehicle wheel alignment measurements. The design of the rig to measure the bushing stiffness and the tensile testing of the suspension bushing is described in section 3.5. The succeeding chapter lays down conclusions based on the findings during wheel alignment measurements.

3.1   Test Vehicles and Conditions

A full vehicle alignment was done on all the vehicles used for this research. Since full vehicle alignment includes measurements of both, front and rear wheels, it is essential to inspect the front and rear suspension for any damage. Any damage in the suspension can result in undesired errors effecting the results of the alignment measurements. A wide range of vehicles were used to study the effects based on

suspension types and suspension stiffness. Vehicles to be included for the research were required to have no visible or evident wear. It was ensured that the bushings were in good condition to eliminate any errors due to bushing deflection. The effect of bushing stiffness on alignment measurements is described in section 3.4. Ball joints were inspected for any measurable deflection to avoid any compliance effects on the wheel alignment measurements. All the suspension members were examined for any damage or visible scrapes.

A wide variety of vehicles were aligned in order to generalize the influence of variables on alignment measurements for all passenger vehicles. Figure 3.1 is a small FWD, 2005 Mini Cooper, test vehicle with a balanced suspension stiffness.

Figure 3.1: Small FWD test vehicle (2005 Mini Cooper).

To study the influence of operator variables on wheel alignment, additional observations required more intensive study on a particular vehicle. Hence, a full sized RWD, 2005 Mercedes E320 CDI, test vehicle was used and may be the most wheel aligned vehicle in North America. The wheel alignment was measured on this vehicle over 160 times. Figure 3.2 shows the Mercedes model used for this research.

Figure 3.2: Full sized RWD test vehicle (2005 Mercedes E320 CDI).

Figure 3.3 shows a SUV, 2007 Acura MDX, test vehicle placed on bearing plates for alignment measurements. In order to study the parameter influence on wheel alignment, the measurement data from the SUV was also included in the data set.

Figure 3.3: The SUV test vehicle (2007 Acura MDX).

The research aimed at providing a correlation between softness of the suspension and the wheel alignment repeatability. In order to study this, two vehicles were specifically chosen due to their soft suspension. These were 1991 Cadillac Coupe

DeVille and 2001 Mercury Grand Marquis. Figures 3.4 and 3.5 show the models of Cadillac and Mercury used for alignment.

Figure 3.4: FWD luxury sedan test vehicle (1991 Cadillac Coupe DeVille).

Although very old for our testing, both vehicles appeared to have been very well maintained and suspension components and bushings were in surprisingly good shape. Cadillac being a 1991 model was in excellent condition and had approximately 87,000 miles on the odometer. The reason to select the Cadillac was its air suspension which helped to examine the influence on wheel alignment due to soft air suspension.

Figure 3.5: RWD luxury sedan test vehicle (2001 Mercury Grand Marquis).

In addition to these vehicles, a luxury sports car was aligned. The intention was to study the influence due to a stiff suspension in RWD sports car. Figure 3.6 shows the RWD sports car used to take alignment measurements.

Figure 3.6: RWD sports car test vehicle (1999 Porsche 911 Cabriolet).

Figure 3.7 shows a UNC Charlotte NASCAR Sprint Cup Race Car which was used because of its stiff suspension and extraordinary +ve 6° LF camber.

Figure 3.7: UNC Charlotte NASCAR Sprint cup race car.

The effect of suspension bushing was studied by taking alignment measurements on a low ride height FWD Coupe, 2005 Toyota Celica. The wheel alignment measurements were taken with old and used OEM bushings, new OEM bushings and polyurethane bushings.The suspension bushing was tested on a tensile testing machine with the aid of a self designed rig. The load v/s displacement plots were used to determine the stiffness of the different bushings used for this research. The wheel alignment measurements taken with different bushings were used to lay down conclusions for wheel alignment measurements influenced by suspension bushings. Figure 3.8 shows the Toyota Celica which was modified to study the suspension bushing influence on wheel alignment.
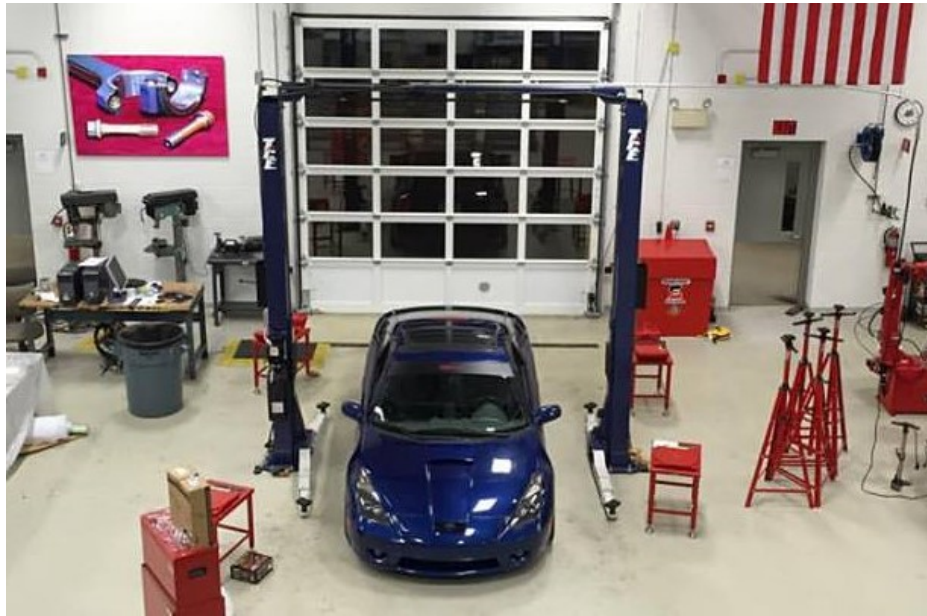
Figure 3.8: Lowered FWD coupe (2005 Toyota Celica).

In addition to these vehicles, a sporty RWD sedan, Lexus IS250 and a RWD Honda S2000 CR was also used to increase the data set and hence get reasonable correlation between suspension stiffness and wheel alignment. All the wheel alignment measurements were logged in an excel sheet with date,time, model, tire pressures, driver and the conditions during the time of measurement. Any changes in the normal test protocol was noted down for future reference. Table 3.1 shows the list of vehicles

used for this research in tabular form.

Table 3.1: Vehicles used for research.

Vehicle Type	Model
Small FWD	2005 Mini Cooper
Full Sized RWD	2005 Mercedes E320 CDI
7 Passenger SUV	2007 Acura MDX
FWD Luxury Sedan	1991 Cadillac Coupe Deville
RWD Luxury Sedan	2001 Mercury Grand Marquis
RWD Sports Car	1999 Porsche 911 Cabriolet
NASCAR Race Car	UNC Charlotte NASCAR Sprint Cup Race Car
Lowered FWD Coupe	2005 Toyota Celica
Sporty RWD Sedan	Lexus IS250
RWD Sports Car	Honda S2000CR

3.2 Hunter DSP700 Wheel Alignment Machine

Wheel alignment helps to reduce tire wear increasing the life and enhance the tire performance. It avoids strange vibrations of the vehicle and maintain stability at all speeds. Wheel alignment is the adjustment of suspension of the vehicle. Wheel alignment is even done to alter the alignment angles other than manufacturer's recommended values to get specific handling characteristic. In motorsports and off-road applications the alignment angles are beyond normal. All the passenger cars require alignment to be done every 50,000 miles or after a car has been in an accident. Wheel alignment ensures the safety of the vehicle by improving stability and unnecessary tire wear.

3.2.1 Wheel Alignment Equipment Details

All the alignment measurements were performed on Hunter Pro-Align DSP700 conventional wheel alignment sensors as shown in figure 3.9. The high speed wireless DSP (Digital Signal Processing) sensors use integrated microprocessors to measure alignment angles [30]. The DSP700 conventional sensors allows rolling compensation providing precise wheel alignment measurements with ease.

Figure 3.9: Hunter DSP700 conventional sensor kit.

The alignment software has an intuitive alignment sequence which provides smooth and easy alignment procedure. It is developed to be used by personnels at all skill levels. The kit is equipped with a pair of long-arm sensors and a pair of short-arm sensors. This system provides reversible setups i.e. interchangeable front and rear sensors to avoid obstructions such as air dams or spoilers. The sensors come with rolling compensation. This provides precise alignment measurements without jacking up the vehicle. The sensors provide continuous runout compensation procedure to ensure accurate alignment angles, even if wheels rotate after compensation. Being a wireless system it has no cables to connect. The sensors are equipped with recharge-able batteries and can be charged when they are mounted on the aligner. The sensors are easy to handle because of its light weight construction and strong magnesium body. The sensors are compatible with all vehicles even with special adapters. Its comes with a sensor locking mechanism to hold the sensors firmly. The alignment values do not change because of its interrupted measurement retention feature. The

following table 3.2 shows the specifications of the sensors.

Table 3.2: DSP700 sensors specifications

Power	3.6vdc (6 rechargeable NiMH AA batteries)
Cordless (standard)	2.4Ghz direct sequence spread spectrum transmitter
Weight	Short toe arm sensor - 2.95 kg (6.50 lbs.)
	Long toe arm sensor - 3.29 kg (7.25 lbs.)
Clamping range	254 to 622 mm (10 to 24.5 in.) [standard]
	711 mm (28 in.) [with extensions]
Wheel base	1778 to 5334 mm (70 to 210 in.)
Treadwidth	1168 to 2286 mm (46 to 90in.)
Sensor body	Impact-resistant rubber
Toe arm	Magnesium

The sensor clamps are ideal for use on wheels without rim lips or when space between tire and rim is limited. The DSP700 sensors utilize self-centering wheel adapter. The wheel adapters have a movable center caster to avoid spoilers and other obstructions. Hunter DSP700 sensors performs quick and accurate wheel alignment measurements as compared to other conventional sensors. The procedure for taking wheel alignment measurements is explained in the following section.

3.2.2   Wheel Alignment Procedure

A proper wheel alignment procedure as recommended by the manufacturer of the equipment was followed consistently throughout the research except the cases with a protocol effect test. The consistency in alignment procedure is essential to avoid undesirable errors and hence provide precise and accurate measurements. The alignment procedure right from the selection of the vehicle in the software to printing the summary of alignment measurements is described in this section.

This section is an overview of an alignment job. The system configuration was not changed between subsequent alignments. The configuration was kept the same for all vehicle alignment measurements. The vehicle is lifted up using the alignment lift and brought down on the stands with turn plates with the wheels properly centered on

the turn plates. It was ensured that the rear wheels were not bound to end plates (for rollover protection). After placing the vehicle on stands the vehicle transmission was put in park and parking brakes were applied to hold the wheels steady. The alignment stands were leveled prior to placing the vehicle to perform proper alignment. The vehicle tire pressures were adjusted to manufacturer's specification. The suspension and steering linkage components were inspected for wear, looseness, or damage.

The first step after starting the software is to enter the customer identification. In this case, the name of the driver and the test number was noted down every time in the "Work Order ID" tab. This ensures the test identification while sorting the measurement database. Figure 3.10 shows the customer identification screen displayed at the start of the alignment software.

Figure 3.10: Customer identification screen [36].

The next step includes selecting the make, model and year of the vehicle under study. After selecting the make of the vehicle, the software lists different models of the car for selection. The next page enlists different trim levels of the vehicle along with the vehicle year. Figure 3.11 shows the list of manufacturers to select from on the first page of the vehicle specifications.
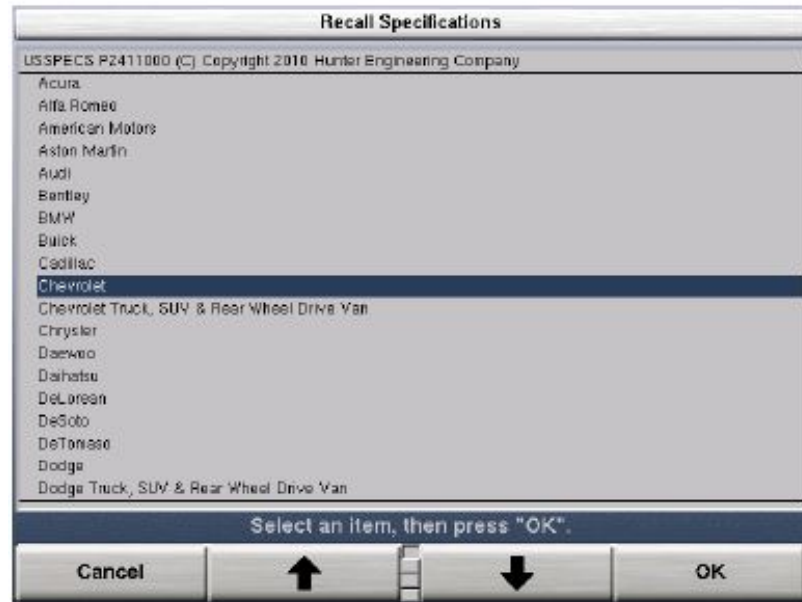
Figure 3.11: Vehicle make selection screen [36].

After selecting the vehicle, the next screen shows the factory recommended alignment values as shown in figure 3.12.

Figure 3.12: Vehicle specifications screen [36].

The sensor heads are mounted on the wheel using a wheel clamp. The wheel adapter is positioned with the two upper rim studs on the outside of the wheel rim

lip as shown in figure 3.13. The adapter adjuster knob is turned as needed to expand the adapter to fit the rim. The two lower rim studs are aligned to grasp the outside of the rim. By turning the adapter adjuster knob, the adopter is firmly gripped onto the wheel. The wheel adapter is lightly tugged to test the security of the installation.
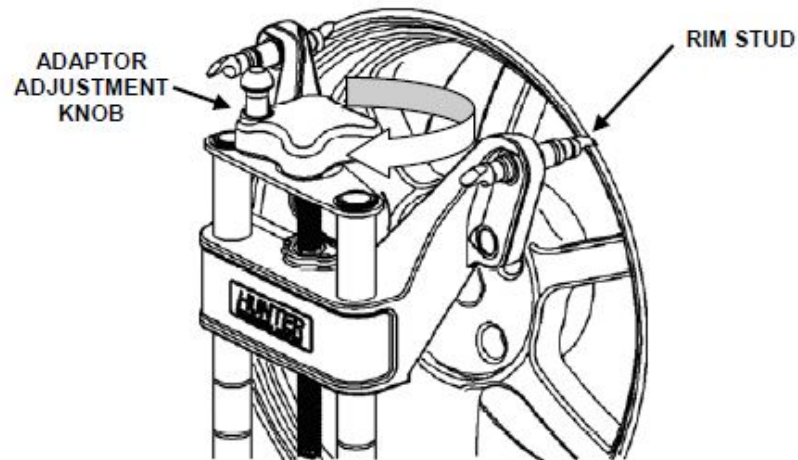
Figure 3.13: Mounting the sensor clamp onto the wheel [36].

After selecting "Measurements and Adjustments" the sensor compensation screen appears as shown in figure 3.14.
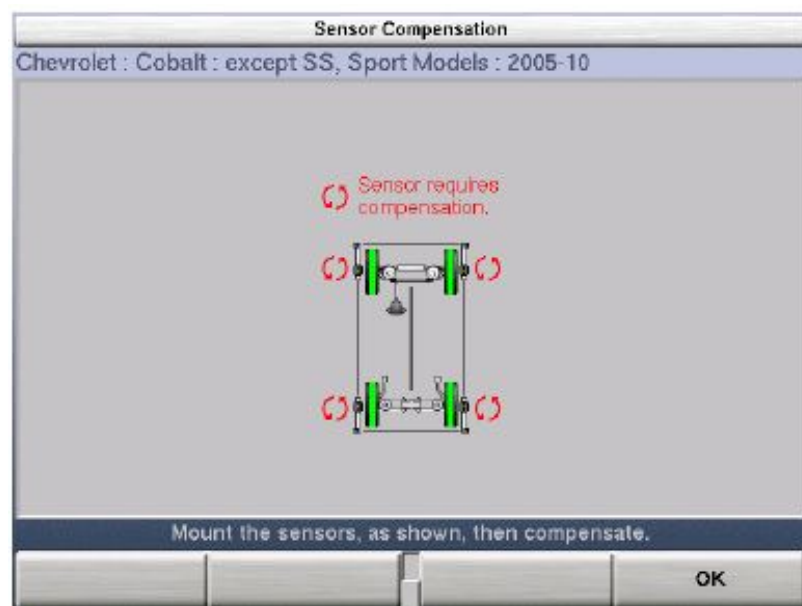
Figure 3.14: Sensor compensation screen [36].

The sensors must be compensated to eliminate errors in angle measurements caused by runout of the wheel, wheel adapter, and sensor shaft. After mounting the sensors, the sensors are turned on and left undisturbed until two outer LED's respond. Sensors can be compensated in any order; however, if a sensor is removed form a wheel, that sensor must be re-compensated when reinstalled. All sensors need not be mounted before starting compensation. The sensor is turned on and any one senor is selected for compensation. The starting position of the wheel adapter does not matter. The middle LED will be on at first position.
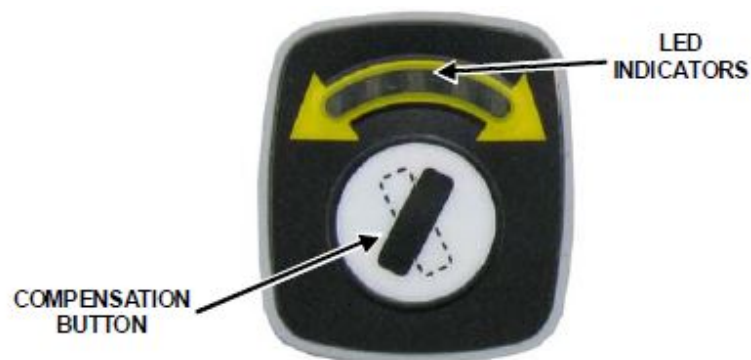
Figure 3.15: Sensor compensation button with LEDs [36].

The sensor lock knob is hand-tightened and the wheel is rotated intil the sensor is level as indicted by the spirit level on top of the sensor. The compensation button is pressed and the sensor is left undisturbed until the two outer LED's begin to blink and middle LED turns off, indicating that the measurements have been stored. The sensor lock knob is loosened and the wheel is rotated 120°, clockwise or counter clockwise, until the middle LED turns on. Again hand tighten the sensor lock knob and rotate the wheel to level the sensor. The compensation button is pressed when the middle LED is on. The sensor is left undisturbed until two outer LED's begin to blink faster and middle LED turns off. The wheel is rotated 120° after loosening the lock knob and the procedure is repeated once again. This time two outer LED's and the middle LED stay on indicating the end os compensation process. The sensor lock knob is now kept loose. After three-point compensation, the wheel maybe rotated to any position

without affecting the alignment measurements. All the sensors should be leveled and unlocked to minimize tilt of the sensors. The vehicle is then lowered on turn plates and jounced to settle the suspension. In three-point compensation, if a previously compensated sensor should require re-compensation, pressing the sensor compensate button twice within four seconds will restart the compensation procedure and retake the first reading for that sensor at this position.

When the sensors have been compensated, the current vehicle alignment measurements are shown as shown in figure 3.16.
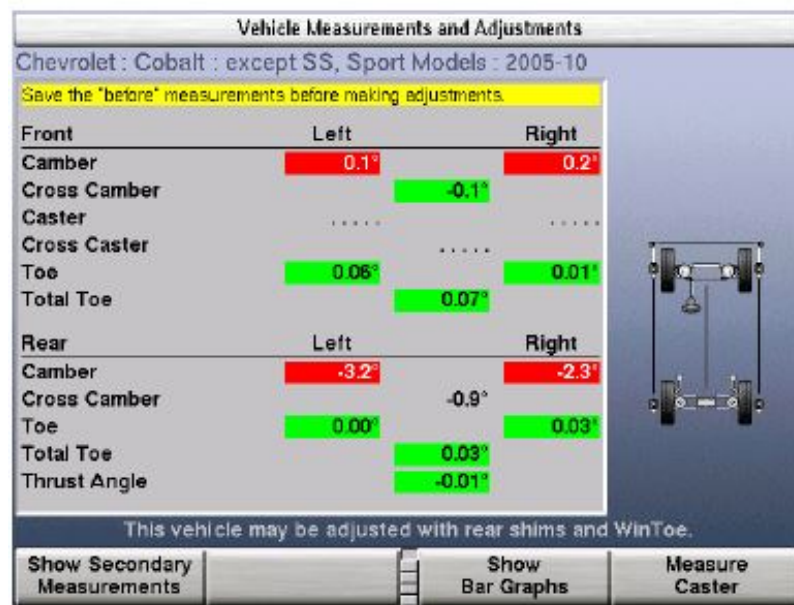
Figure 3.16: Current alignment values [36].

Pressing the "Measure Caster" button changes the screen to "Caster and S.A.I Measurement" screen. The wheels are steered following the instructions shown on the screen. When the caster has been measured, the screen changes back to "Vehicle Measurements and Adjustments" screen but now with caster angle values. The measurements are saved using the save button. The vehicle is jounced and the wheels are steered straight ahead and then button "Ready" is pressed as shown in figure 3.17. When the measurements are stable, the program saves the measurements and the screen changes back to "Vehicle Measurements and Adjustments" screen.
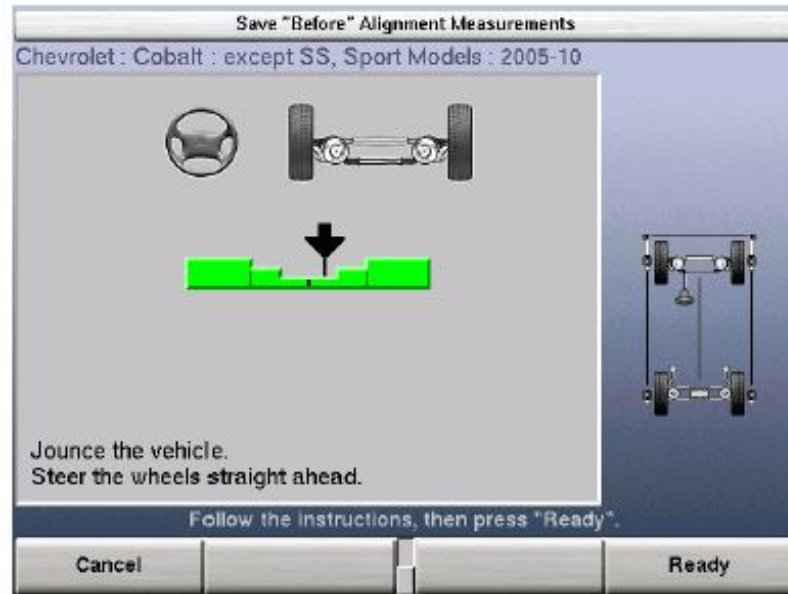
Figure 3.17: Saving alignment measurements [36].

After the front and rear alignment is complete, an alignment summary is printed by pressing "Print". The vehicle is jounced and the wheels are steered straight ahead until the bar graph indicates a centered position as shown in figure 3.18.
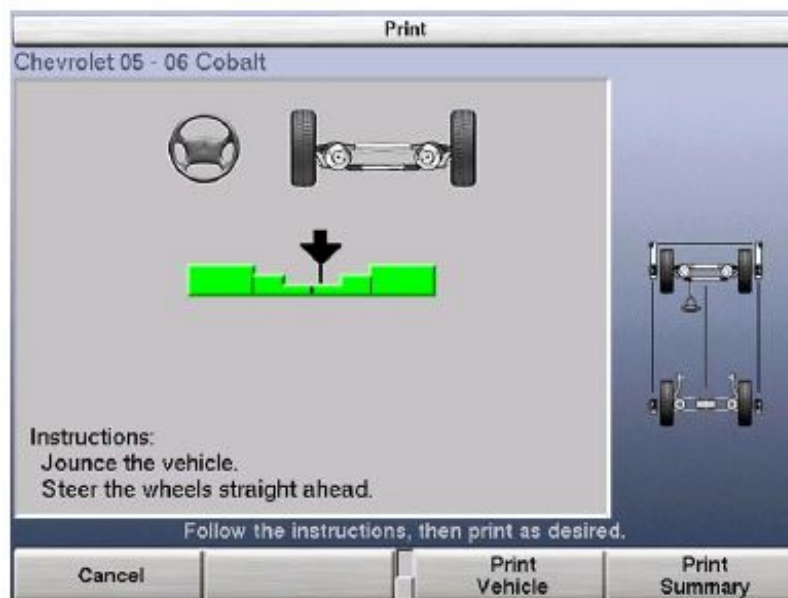
Figure 3.18: Printing the measurements [36].

As the arrow touches the center of the bar graph, "Print Summary" button is
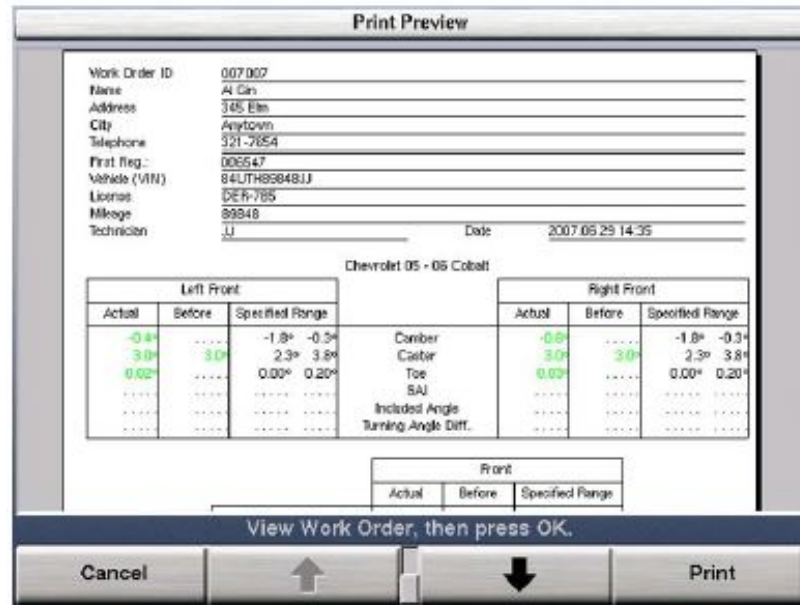
Figure 3.19: Print preview of alignment measurements [36].

pressed and the screen changes to "Print Preview" screen as shown in figure 3.19. The sensors are then removed from the vehicle and the aligner is reset.

3.3   Test Protocol

The wheel alignment measurements of all vehicles were recorded following the procedure described in section 3.2.2. In most cases, except for a protocol effect test the vehicle was lifted off the wheel stands between each measurement and jounced to settle suspension after being rested back on the stands. To avoid wedge effects, the top of the bearing plates were leveled with an LS Starett 98Z-12 spirit level, which has a resolution of 80-90 arc seconds or a levelness of 0.6mm (0.025") on a 1.4m (55") track [37]. Digital compensation was performed on DSP700 sensor heads to correct the misalignment between wheel bearing plane and mounting flange plane prior to each test. Caster sweeps were performed during all the alignment measurements. Prior to the recording of the final readings the vehicle was jounced again to settle the suspension [1] [2].

Several measurements were made to determine the accuracy of the alignment

equipment before studying the parameters influencing the alignment measurements. To assess the repeatability measurements of DSP700 sensors a rigid aluminum test fixture was developed as shown in figure 3.20.

Figure 3.20: Aluminum alignment head test fixture.

The DSP700 heads insert into a drilled and $\varnothing15.00$mm ($\varnothing0.5906$") reamed mounting hole in the frame fixture attachment. This design eliminated errors due to wheel mounting clamp and simplified the reverse head measurements described in further part of the section. The DSP700 sensor heads cannot read if the heads are held are too close together and hence the fixture was made about 1.1m x 1.8m. As seen in figure 3.20 the fixture is supported on three legs defining a single plane hence avoiding any external twisting of the aluminum frame. The average standard deviation for the test frame for both camber and toe were about 0.01° which is the resolution of the DSP700 sensor heads. This ensured that the equipment was calibrated as per requirement [38].

In the next test, the heads of the alignment were reversed and measured at different locations. The left front (LF) wheel head was moved to right rear (RR) and the camber and toe changes were measured. All the heads were repositioned 180° from their normal locations. The average change in reverse head measurements was 0.02° in camber and 0.03° in toe measurements. The reverse head measurements showed

that variance is related more to fixturing than sensors, and that the number changes are small [38].

The Mercedes was repeatedly used for special alignment tests. Over the period of research work, the alignment of the Mercedes was measured over 160 times. This vehicle was used to study operator influence, wedge influence, date and time influence, tire pressure influence and front toe preload influence on alignment measurements.

The measurement of one variable influence was the levelness of the bearing plates. The aim was to study the effect of a bearing plate that is higher or lower than the horizontal plane of other plates. A simple example of this is that if the vehicle is driven onto ramps that have the left ramp one degree higher than the right ramp, then all of the left side camber angles will be one degree more negative and all of the right side camber will be one degree more positive [2]. The Mercedes E320 CDI was used to evaluate the alignment equipment. The statistical data from the control tests was used as a comparison to the variable test condition results. Most of the measurements were done by the same operator.

In the first test, everything was kept at normal conditions as mentioned in the procedure described above and the control was with the driver. This was considered as "no wedge" condition, as the wheel was not displaced up or down and had all tire pressures at the manufacturer's recommended values. The cross weight or wedge is defined as the LR and RF weights over the total vehicle weights and it was not perfect 50% but rather 50.2%. Any wedge at this point is a result of vehicle suspension variability, and was considered small compared to other measurements.

The wedge effect on alignment measurements was tested by inserting a 3/4" (19mm) plate between the bearing plate and the LR tire of the Mercedes E320 CDI. Load cells were placed between the wedge plate and the tire so that the wedge can be measured. This test was used to study the impact of not having a flat platform onto which the alignment is measured.

The influence of tire pressures on alignment measurements was also performed on the Mercedes. In this protocol, the tire pressures were varied over a range from the recommended values to create a wedging effect on the vehicle. In one of the cases, we increased the wedge to 56.3% by increasing the LR and RF tires to 50 psi and dropped the LF and RR to 15 psi. In the other protocol, the wedge was reduced to 45.7% by increasing the LF and RR tire pressures to 50 psi and dropped the LR and RF to 15 psi. Tire pressure had the most significant influence on wheel alignment measurements.

To explore more about the influence of tire pressures on wheel alignment measurements we studied the one tire pressure error impact. In this case, the tire pressure on LF, LR, and RR tires was increased to 50 psi and dropped the RF tire pressure to 15 psi which resulted in a reduced wedge of 47.6%. In other case, we increased the RF, LR, and RR tires and dropped the LF tire pressure to 15 psi which resulted in an increased wedge to 53.6%. The impact of only changing one tire pressure resulted in most interesting phenomena on alignment measurements.

Mercedes has a special procedure which requests that the front suspension have a Toe-Out preload force (at the front of the front tires) during the alignment. To evaluate the effect of this, we manufactured a preload fixture with a measured force and then varied the force and recorded the effect on Toe. The assumption is that as the suspension bushings wear, a slight preload will offset the Toe outward. For an 1800kg vehicle, a corner weight would roughly be 450kg and the rolling resistance would then be around 1.5% or 7kg. If the tire pneumatic offset outward is about 25mm and our preload device is located 160mm forward of the centerline, then to get a vertical axis moment similar to what the tire rolling resistance provides on the highway, we estimate a need to provide a lateral force of 1kg. To bracket this force and evaluate the need for the special Mercedes procedure, we used a range of 0 kg to 5 kg force in one kg increments pushing out on the front of the front tire directly

below the lower front bodywork (160mm forward of the centerline) [1].

Some vehicle manufacturers request that a car be unloaded and some request a load be installed in the vehicle. We did a comparison test on the Mercedes E320 CDI where we did some tests unloaded and some with a 100kg driver. This protocol helped us study the impact of additional weight such as driver weight, fuel tank level, etc. on wheel alignment measurements.

We measured the alignment angles of vehicles with a soft and stiff suspension to study the influence of suspension stiffness on measurement repeatability. We measured the alignment angles for a NASCAR Sprint Cup Car and Porsche 911 Cabriolet to study the repeatability of measurements on stiff suspensions. While to understand the repeatability of measurements on soft suspension we measured the alignment of a Cadillac Coupe DeVille with air suspension and Mercury Grand Marquis. All the measurements were recorded using the normal test procedure.

The next thing to understand was the impact of bushing stiffness on wheel alignment measurements. For this purpose, we used a Toyota Celica with a low ride height for research. We measured the alignment angles with three different front suspension bushings. The three bushings fitted were old and used OEM rubber bushings, new rubber bushings and polyurethane bushings. The stiffness of the bushings was measured using a tensile testing procedure and is explained in section 3.5. In this case as well the normal alignment procedure was followed.

3.4   Design & Manufacturing of Test Rig for Measuring Bushing Stiffness

The objective of designing a test rig was to make the control arm available for measuring the bushing stiffness by using suitable arrangements on the Instron machine. The control arm was fixed on the base plate using the cylindrical bushing end and fixing the bushing free end to the strain gage side of the Instron machine. The ball joint end of the control arm was kept to hang freely. The test rig was designed so as to ease the manufacturing process and be cost efficient at the same time.

The design process started with a rough sketch of the control arm in SolidWorks with approximate dimensions. This is was done to get a rough idea of the test rig design. The bushing stiffness measured was of front left lower control arm of a Toyota Celica as shown in figure 3.21. The rough sketch of the control arm formed the base for designing the test rig.

Figure 3.21: Toyota Celica control arm.

The purpose of design of the test rig was to hold the control arm irrespective of the length of the arm. So for this reason the test rig was designed in two different parts. The test rig design consisted of a base plate assembly and strain gage attachment assembly. The direction of loading was not the main concern as the stiffness of the bushing was to be measured and not the control arm strength. When the control arm articulates the bushing gets twisted in a direction depending upon the load, jounce or rebound intensity of the suspension. Hence the bushing stiffness is more important rather than the direction of the load.

The base plate was designed using a quarter inch mild steel sheet metal. The plate was strong enough to stay firm since only the bushing stiffness was to be measured. The bolt pattern to fix the base plate to the Instron machine was recorded from the
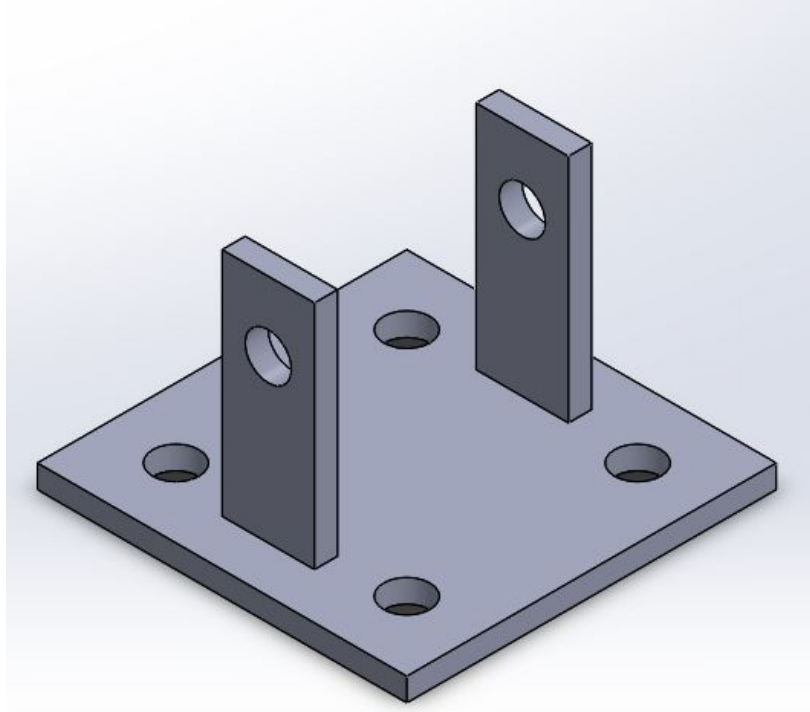
Figure 3.22: Base plate of the test rig.

crosshead of the Instron machine. All the three pieces of the base plate were cut using a iron worker machine including drilling holes. The three pieces were welded together using TIG welding and assembled as shown in figure 3.22.

The second part of the test rig was designed to attach the bushing free end of the control to strain gage end of the Instron machine. The bushing free end of the control arm was bent at angle of 10° from the normal plane. In order to keep the loading in vertical direction and avoid twisting of the bolts the attachment was designed at an angle 10° to the counter the effect of the angle on the control arm. This end of the suspension had three holes in a triangular pattern. A rough sketch of the pattern was used to model the holes on the attachment. Here again all the pieces were quarter inch mild steel sheet metal cut to dimensions using an iron worker, The cylindrical bar was welded at the top using TIG welding to fit the attachment on the Instron machine. Sidewalls were attached to give more rigidity to the structure as shown in

figure 3.23a and 3.23b.
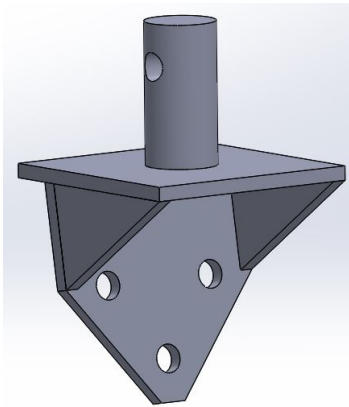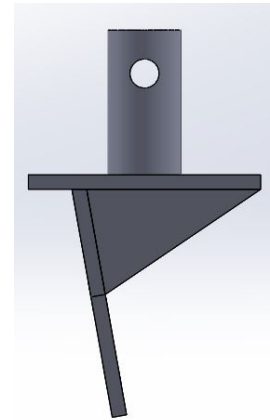
(a) Isometric view. (b) Side view.

Figure 3.23: Attachment to connect control arm to strain gage.

The two parts shown above together forms the test rig and was used to measure the stiffness of the bushing. The two parts were assembled in SolidWorks at an approximate distance equal to the length of the control arm to check the compatibility as shown in figure 3.24.
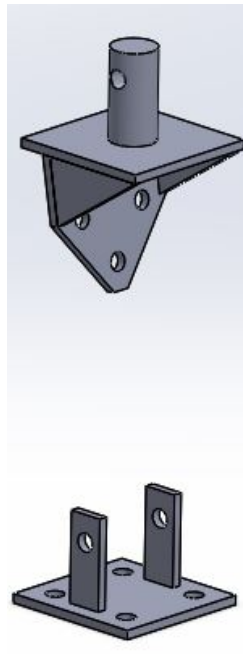
Figure 3.24: Test rig assembly.

3.5   Measurement of Bushing Stiffness

This section of the chapter describes the measurement procedure of bushing stiffness using the tensile testing machine and also gives a brief description of the Instron 4400 R series universal testing machine.

3.5.1   Overview of the Instron Universal Testing Machine

Instron 4400 R series universal testing machine is used for this research part. This machine is used to test the tensile and compressive strength of variety of materials. It consists of a load frame to mount the specimen and test it for tensile or compressive strength. The control panel of the machine assists the calibration and test setup process while testing.

The interaction with the machine is done through a front control panel with various selection buttons. The machine setup is done through a software installed on the desktop which provides real time results in the form of graph including load applied and strain on the specimen. All the results can be stored in the form of graphs and text file containing load values and strain. The crosshead drive and control system are responsible for compressive and tensile loading of the specimen. The strain gages at the top of the machine are used to determine the loading on the specimen [39].

The Central Processing Unit (CPU) is used to control the operation throughout the machine during the testing period. The front control panel is used to program the speed of the crosshead and also gives manual control of the crosshead position. The actions such as stop, return or cycle for the crosshead can be controlled by the front control panel [39].

The strain gages along with load sensor conditioner provides output to the CPU and it allows calibration and balance procedures to be performed automatically once initiated from the front panel.

The rear panel consists of all the cables from the recorders, load cells and strain measuring devices. The console receives its power from an external AC supply which

is converted into DC supply in the load frame.

3.5.2   Procedure for Measuring Bushing Stiffness

The stiffness test was performed on three different bushings using the same setup
and control arm. The test rig designed as explained above was used to attach the
control to the machine for testing. Figure 3.25 shows the test setup and the attachment
of the control arm to the rig and the machine for testing the bushing stiffness.

Figure 3.25: Bushing stiffness test setup.

The test rig was designed in order to simplify the test setup and escalate the test
procedure. The base plate of the test rig was fixed to the crosshead with four bolts

to sit firmly on the crosshead. The control arm was attached to the top attachment fixture with three bolts before attaching to the machine. The crosshead was displaced to accommodate the control arm and the top attachment fixture between the crosshead and the strain gage of the machine. The control arm was then fixed within the extension limit using a single long bolt at the top and at the bottom as shown in figure 3.25.

After fixing the control arm and the test rig between the crosshead and the strain gage, the initial extension between the grips was set to zero using the G.L reset key. This ensures that the initial extension in the bushing is zero. Load calibration was done to ensure that the load displayed on the control panel is adjusted to zero at the start of the test. Using the desktop software, the tensile testing method was selected which ensured unidirectional loading of the bushing and the return cycle of the crosshead was with no load. The maximum test load was set to 1000 lbf and the crosshead speed was set to 0.1 in/min. The data was recorded at the rate of 20 pts/sec. After recording the test data, the file was saved in text format. 10 tests were performed on a one bushing and was repeated for the other two bushings. The graph of Load (lbf) vs. Displacement (in) was plotted from the recorded data as shown in figure 3.26.
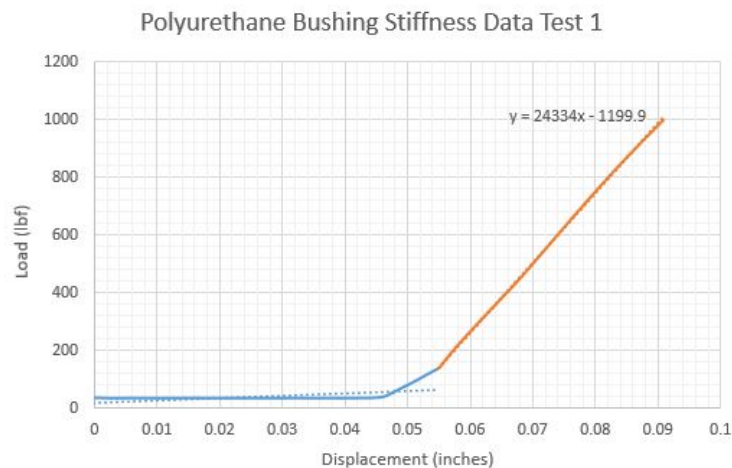
Figure 3.26: Bushing stiffness test data graph.

Figure 3.26 shows one test data for a polyurethane bushing. As such 10 different graphs were plotted from the tests performed for polyurethane bushing. In the graph, the blue data curve is not considered for calculating stiffness as it represents the the slack present in the test assembly.The orange curve represents the bushing stiffness and a linear trendline is derived from the curve. The equation of the trendline is determined in terms of load and displacement. The slope of the trendline gives the stiffness of the bushing under test. The following table 3.3 gives the stiffness of the three bushings and all the tests performed.

Table 3.3: Bushing stiffness test data

Test No.	OE Bushing Stiffness (lbf/in)	Polyurethane Bushing Stiffness (lbf/in)	Old OE Bushing Stiffness (lbf/in)
1	18134	24066	13876
2	18385	24102	13876
3	18691	24152	13822
4	18741	24203	13815
5	18995	24257	13804
6	19085	24291	13844
7	19144	24301	13834
8	19217	24324	13866
9	19258	24307	13885
10	19268	24334	13862
Average (lbf/in)	**18892**	**24234**	**13848**
Average (N/mm)	**3308**	**4244**	**2425**
Standard Deviation	**2.1%**	**0.4%**	**0.2%**

Table 3.3 shows the test data of three bushings tested and gives the average value of the stiffness of all ten tests performed on each bushing in lbf/in and N/mm. As expected the polyurethane bushing has the maximum stiffness than the other two. The old OE bushing due to wear and tear over its service life has the lowest stiffness. These bushings were used to study the influence of bushing stiffness on wheel alignment according to the test protocol described earlier. The conclusions of all the tests performed for wheel alignment are laid down in the following chapter.

CHAPTER 4:   RESULTS AND CONCLUSIONS

The aim of this research was to provide a systematic and accurate way of wheel alignment of a vehicle by eliminating undesirable errors due to operator and suspension variables thus enhancing vehicle stability and handling characteristics, and reducing tire wear. The output of this research was completely based on experiments performed on different vehicles with a consistent wheel alignment procedure for each of its test protocol. The results of the wheel alignment measurements carried out and its conclusions are described in the following sections.

4.1   Results

The measurements taken are analyzed to calculate the standard deviation (SD) of the values for camber and toe measurements. The standard deviation of measurements of each set of test is compared to the average standard deviation of all the measurements the study. Furthermore, the results of special alignment tests, the results of operator influence and variation of measurements with time are presented.

4.1.1   Vehicle Influence on Alignment Variation Results

Wheel alignment of all the vehicles mentioned in section 3.1 was measured to characterize the vehicle dependence on alignment variables. All the vehicles are equipped with an anti-roll bar on both their front and rear suspensions, fully independent coil spring suspension, and rack and pinion steering except the NASCAR Sprint Cup Car.

4.1.1.1   Full Sized Sedan Results

A 2005 Mercedes E320 CDI was the reference full sized four door sedan. It has a rear wheel drive and a five link rear suspension. The front suspension is similar to double wishbone suspension with each arm having their own ball joint making a pivot

location outboard in the brake disc.

The average standard deviation of the 40+ camber measurements for the CDI was 0.04° which was almost twice the 0.025° average of all the measurements in the study. The average SD of the toe was about the same as the average test SD.

4.1.1.2   Small Front Drive Car

A 2005 Mini Cooper with a MacPherson strut front suspension and trailing arm with two lateral links rear suspension was used as small front drive car. The average SD of 10 camber measurements was 0.026° which is close to the 0.025° average of all measurements in the study. The SD of the toe measurements was 0.033° which is close to twice the 0.017° average SD of all the measurements in the study.

4.1.1.3   Sports Cars

One of the sports car used was a 1999 Porsche 911 Cabriolet with a MacPherson strut front suspension and a driven multi-link rear suspension. The average camber SD of 0.008° and toe SD of 0.012° are both about half the test mean SD (low variability of measurements).

The second sports car was a 2012 Honda S2000 CR, having a unique racing alignment with over 3.0° of negative camber. It has a double wishbone front suspension and a multi-link rear suspension. The average SD in camber of 0.039° the S2000 has a higher value than the test average but with average camber numbers of this car of 3.0° it is expected that there is correlation between magnitude and variability. Following this logic, the average SD in toe is 0.10° which is measurably less than the test average of 0.017°.

4.1.1.4   SUV

A four wheel drive 2007 Acura MDX with a strut front suspension and multi-link rear suspension was used for SUV measurements. The average camber SD of 0.006° is mush smaller than the test average and average toe SD of 0.018° is about the same as test average.

4.1.1.5   Race Car

A NASCAR Sprint Cup car used to take measurements for this category. It has no rubber bushings on a double wishbone front suspension and a live beam axle rear suspension with longitudinal giant rear anti-roll bar. The wheel alignment was like a normal Sprint Cup car with huge left turned bias front camber, the alignment was plagued by a strong steering torque to the left. A considerable strength is required to hold the steering straight without the engine running.

The LF suspension has a very large static camber of $+6°$;however, due to stiff suspension, the average SD was measured to be very low $0.014°$ for camber and $0.013°$ for toe.

4.1.2   Operator Influence on Wheel Alignment Measurements

The operator influence was assessed by calling upon several operators to perform wheel alignment measurements on the Mercedes E320 CDI. Figure 4.1 shows the sensitivity to one operator who made the measurements at steps #6 and #8. The variation was determined to be caused by the bearing plates bound up at the extreme of their freedom of motion. Step #7 was performed with no driver in the car. The variation was determined due to the difference in weight with no driver present.
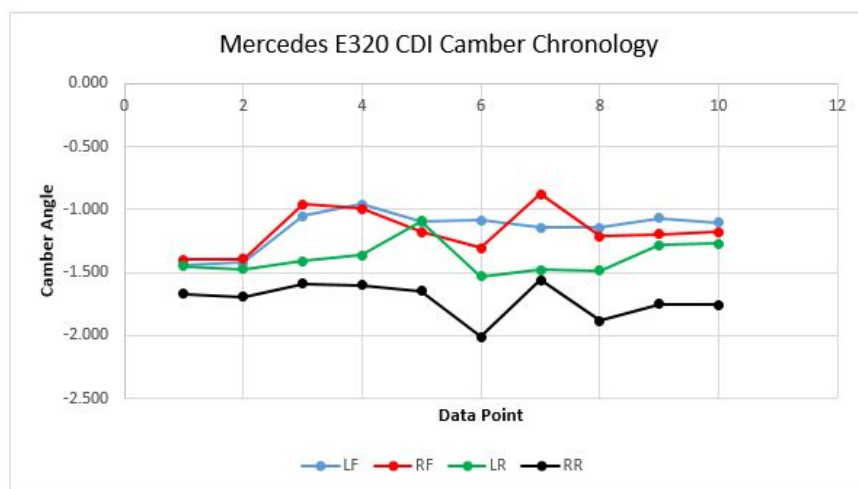
Figure 4.1: Mercedes camber chronology (Test 7, April 2015, was with no driver in the car).

The results show that the wheel alignment measurements can be influenced by the operator performing wheel alignment, be it a professional or an amateur. The binding up of bearing plates is one of the effects an operator influences the wheel alignment measurements. Other reasons such as the ratcheting effect of the tire against the front bumpers of rear stands (to prevent the car from rolling off), improper runout compensation of sensor heads or saving the measurements without the steering pointing straight ahead can also cause variation in measurements which are influenced by the operator.

4.1.3 Variation Wheel Alignment Measurements with Time

In one year time frame of the measurements, very little drift was found in either the vehicle or alignment equipment. Measurements on the Mercedes or Porsche were recorded over a period of one year.
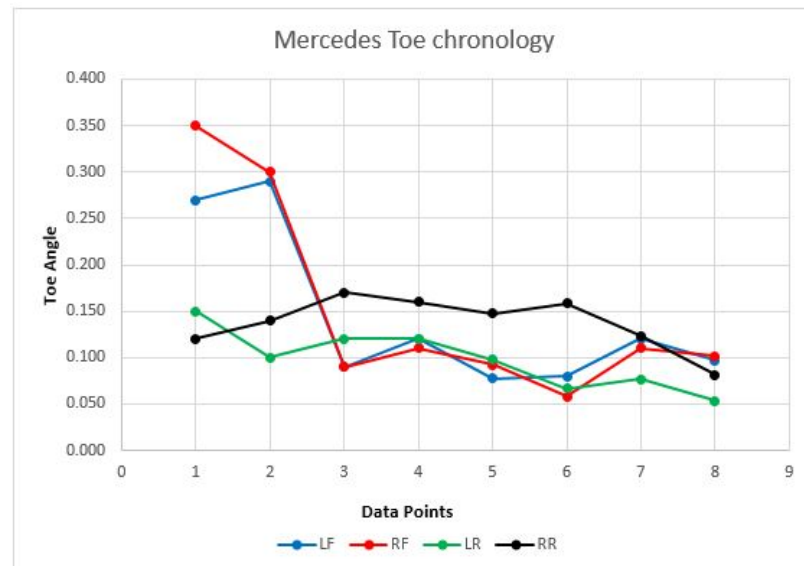
Figure 4.2: Mercedes toe variation with time.

Figure 4.2 shows the toe-in for Mercedes and step #3 is a toe adjustment done in August 2014 and proved to be stable after that. Step #8 shows little change in toe readings 11 months later. As per the figure 4.1 shown in section 4.1.2, which is a camber evolution of the Mercedes throughout one year period. Step #8 is test with

no driver and hence less weight in the car.
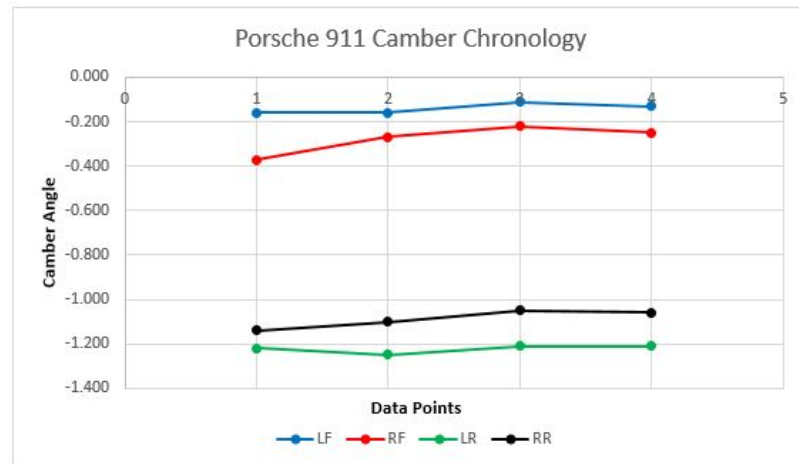
Figure 4.3: Porsche camber variation with time.

Figure 4.3 shows the Porsche camber evolution from August 2014 through May 2015. From the plots shown, very little change was observed in this time frame. These results conclude that wheel alignment is a stable thing. On the Mercedes E320 and Porsche 911, wheel alignment measurements changed very little over the fourteen months.

4.1.4 Special Alignment Test Results

To study the variation in wheel alignment apart from the normal procedure followed during research, we recorded measurements based tire pressure influence, suspension stiffness and bushing stiffness. The results for same are described below.

4.1.4.1 Mercedes Toe and Weight Preload Test

As explained earlier in 3.3 Mercedes has a special procedure which requests that the front suspension have a toe-out preload force at the front of the front tires during the alignment. The results did not demonstrate a need for this special procedure. Rather than make a table of results, a summary is that the total front toe-in was $0.11°$ $\pm0.01°$ with no particular trend in the data recorded. However, it can be predicted that toe preload test would differ at the level of suspension bushing wear. To sum it up, no

toe influence was measured in this test; however, this protocol may become more important on a heavily worn vehicle.

Some vehicle manufacturers request that a car be unloaded and some request a load be installed in the vehicle. We did a comparison on the Mercedes E320 CDI where we did some tests unloaded and some with 100kg driver. We did not see much change in the SD; however, as expected, we did see a change in average camber values. We found that although the left side only changed 0.03°, the right side camber increased (more neagative) by 0.40°. We did not see much change in the toe values which is surprising considering rear bump steer effects (however, the driver doesn't add much weight to the rear suspension).

4.1.4.2 Wedge Influence on Alignment Results

The wedge effect on wheel alignment was measured by inserting a 19mm (0.75") plate between the bearing plate and tire of the vehicle. The data points recorded under normal procedures and under wedge conditions are described in the following graphs.
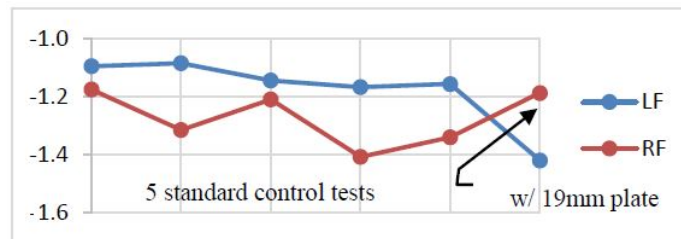
Figure 4.4: Front camber with 19mm plate under LR tire in last case.
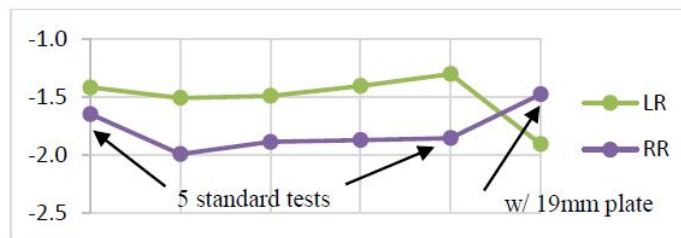
Figure 4.5: Rear camber with 19mm plate under LR tire in last case.

Figure 4.4 shows the effect on the front camber and figure 4.5 shows the result on rear camber. In both these figures, cases 1, 2, 3, 4, and 5 are previous runs with standard conditions and case 6 is with the 19mm block under the LR tire. Although this is semi-intuitive, (lean the car a degree, all of the cambers change a degree) it does not show the impact of not a flat platform onto which the alignment is measured. That is, the changes shown in figures 4.4 and 4.5 are the result of just one wheel being non-level. Furthermore, with that one wheel platform high, the right side camber changes 0.3° positive and the left side changes 0.4° more negative. For accurate camber and toe measurements, it is important the bearing plates are level and coplanar.

4.1.4.3 Tire Pressure Influence on Alignment Measurements

The Mercedes E320 CDI sedan was used to evaluate the equipment. We used the statistical data from our control tests and compared them to the variable test condition results. Most of these measurements were done by the same operator in the car. The following table 4.1 shows the effect of tire pressures on cross weight which were used as test conditions for this study.

Table 4.1: Tire pressure effect on cross weight (wedge).

Test No.	LF (bar/psi)	RF (bar/psi)	LR (bar/psi)	RR (bar/psi)	Wedge %
1	2.2/32	2.2/32	2.3/34	2.3/34	50.2%
2	2.2/32	2.2/32	2.3/34	2.3/34	52.4%
3	1.0/15	3.4/50	3.4/50	1.0/15	56.3%
4	3.4/50	1.0/15	1.0/15	3.4/50	45.7%
5	3.4/50	1.0/15	3.4/50	3.4/50	47.6%
6	1.0/15	3.4/50	3.4/50	3.4/50	53.6%

Several influences were measured but the most significant was the inflation pressure of the vehicle tires. Figures 4.6 and 4.7 shows the effect of inflation pressure on camber angles. The data points 1 to 4 were all standard tests on different dates. On the data point 5 (test #3 in table), we increased the wedge to 56.3% by increasing the LR and

RF tires to 3.4 bar (50 psi) and dropped the LF and RR to 1.0 bar (15 psi). On data point 6 (test #4 in table), we reduced the wedge to 45.7% by increasing the LF and RR tires to 3.4 bar (50psi) and dropped the LR and RF to 1.0 bar (15 psi).
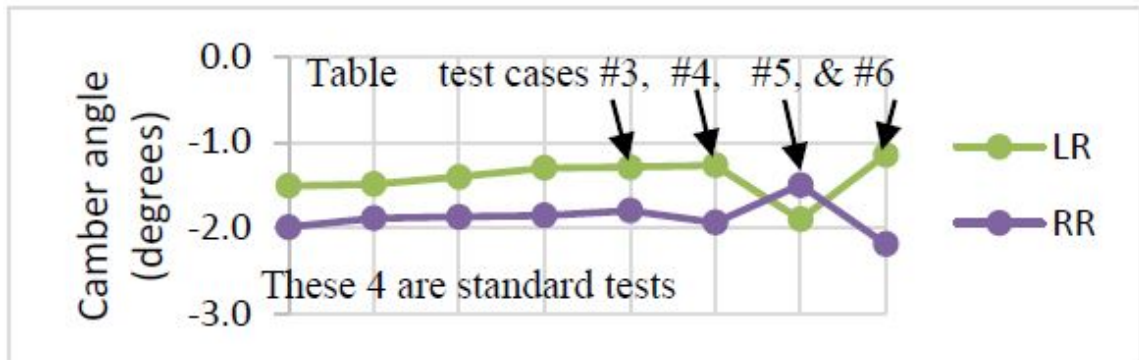
Figure 4.6: Inflation pressure impact on rear tire camber.
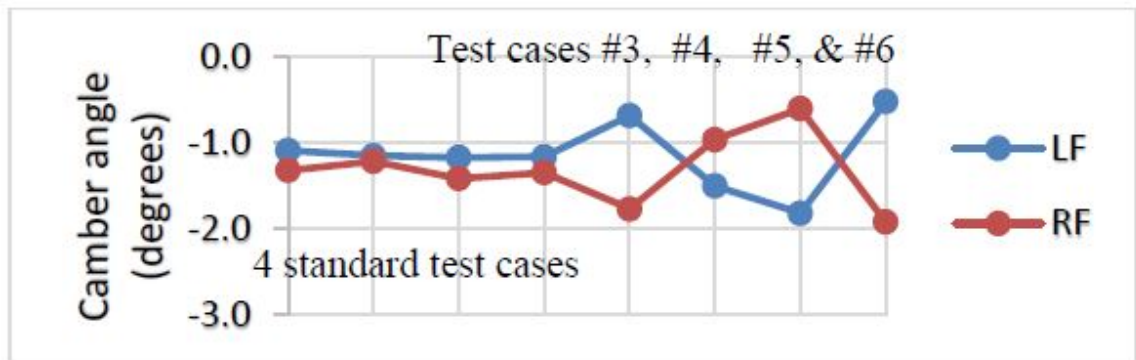
Figure 4.7: Inflation pressure impact on front tire camber.

The average variation in front camber measurements is 0.06° for each of the standard test cases. For table test case #3 (56.3% wedge) and table test case 4 (45.7 % wedge) the error rose to 0.41° and for the rear cambers, the average camber was only 0.11°. For accurate measurements, it is important that wedge not be introduced by two low tire pressures.

The most interesting phenomena was the impact of only changing one tire pressure. On table test case 5, we increased the LF, LR, and RR tire to 3.4 bar (50 psi) and dropped only the RF to 1.0 bar (15 psi) which resulted in a reduced wedge of 47.6%.

On table test case 6, we increased th RF, LR, and RR tires to 3.4 bar(50 psi) and dropped onlt the LF to 1.0 bar (15 psi) which resulted in an increased wedge to 53.6%. In these single tire pressure error cases, the average error in front camber angles rose to an outstanding 0.66°, and the average error in rear camber angles rose to 0.37°. These were both higher than either of the two previous cases.

This means that a single tire pressure error can have a stronger influence on he alignment results than even two diagonal tires being underinflated. This may be only valid for a front tire pressure error and only influence the front tire camber angles. The average toe angle in toe angle also showed remarkable changes but some toe adjustments were made during the previous months and the confidence is less.

4.1.4.4 Influence of Suspension Stiffness on Wheel Alignment

Prior to recording wheel alignment measurements, our assumption was that stiffer the suspension, the more repeatable the alignment would be. To test this more thoroughly, we located vehicles with reputations for very softly sprung suspensions.

We located a 2001 Mercury Grand Marquis for this test. the front suspension is a double wishbone style mounted to a sub-frame. The rear suspension is a beam axle with trailing arms and a Watts linkage for lateral control. The results did not support the softness impact on the measurements. The average SD in camber for this vehicle was only 0.016° (about the mean of our vehicle measurements). Obviously, a beam axle car should not have much rear camber change; however, this vehicle has a front sub-frame and it is suggested that the suspension bushings may not be as soft as previously thought. That is, softness may be between the sub-frame and the chassis. This may support why this vehicle does not follow the previously measured influence of suspension softness on low repeatability measurements.

The second soft suspension vehicle for this test was a 1991 Cadillac Coupe DeVille. This vehicle has a strut suspension both in front and at the (air bag) rear suspension. The average camber SD measured by two operators was 0.030° or about 25% higher

than the mean of all values measured.

The result is that although the earlier results suggested that for a modern vehicle, the repeatability of suspension alignment is not strongly affected by the softness of the suspension.

4.1.4.5   Influence of Suspension Bushing Stiffness

The suspension stiffness did not produce any reliable results showing any influence over wheel alignment measurements. The next step was to check the influence of bushing stiffness on wheel alignment measurements. For this test protocol we located a 2005 Toyota Celica with a low ride height and having a MacPherson strut suspension. All the measurements were recorded using the same operator. One set of readings was taken with with OEM bushings already on the suspension arms. Other set of readings was recorded with new control arms having OEM bushings. And next set of readings was taken using the polyurethane bushings. Due to the complexity of the suspension design only front control arm bushings were replaced and the rear control arm bushings were left unchanged. However, we managed to change the anti-roll bar bushings at the rear. All the three bushings were tested for its stiffness on a universal testing machine as described in section 3.5.

Since we changed only the front bushings, the results presented only reflect the influence on front wheel measurements. The average SD for LF camber with old OEM bushings was 0.030° while for the RF camber was 0.029° both being a little over the average SD of all the test measurements. The results with new OEM bushings showed similar results but with a little lower standard deviation. The average SD for both LF and RF camber was around 0.022° which was almost close to average SD of all the test measurements. The most interesting results were reflected in the tests with polyurethane bushings. The LF camber had an average SD of 0.013° and that of RF camber was 0.017° almost half of the results for OEM bushings. Although no exceptional results were found in the toe angle of the vehicle and hence it is not

appropriate to comment on toe measurements.

The results depict a slight hint about the relationship between the bushing stiffness and wheel alignment measurements. Although it is true that wheel alignment angles are highly effected by suspension bushings in dynamic conditions. These results lay a platform for researching more about static wheel alignment measurements effected by suspension bushings. One of the reasons can be assumed is the compliance offered by bushings under loaded conditions. Although the suspension linkage compliance is considered while suspension design, there is a need to consider the bushing compliance during design. Bushing selection is actually a trade off between the comfort and ride. Considering these factors in mind, the wheel alignment variation can be reduced to provide better stability and handling characteristics.

4.2 Conclusions

Several things do not seem to make a difference in wheel alignment accuracy. The stiffness of bushings was measured to have an influence on measurements while the suspension stiffness does not have extraordinary effects on the measurements recorded. Another result of interest is that the standard deviation does not appear to be related to the static alignment angles. For example, the static left front camber for the NASCAR cup car is a large 6.61° but its standard deviation is a small 0.019°. Similarly, the left front camber on the Honda S2000 CR is -3.19°, but its standard deviation is 0.046°. Wheel alignment measurements can be influenced by many factors. In this work, we measured wheel alignment 300+ times and evaluated vehicles, protocols, measurement equipment, and time. Mercedes requires a toe-out preload force on the front tires but we did not measure an effect and suspect this may be more important on older high mileage cars. We also measured two vehicles over a year and found little change the commenting on the stability of vehicle suspension alignment and on measuring equipment stability. The following tables provide a summary of data recorded throughout the research.

Table 4.2: Standard deviation of camber and toe by vehicle.

	Camber Standard Deviation					Toe Standard Deviation				
	LF	RF	LR	RR	Average	LF	RF	LR	RR	Average
Mercedes E320	0.030	0.021	0.041	0.031	0.031	0.021	0.023	0.028	0.026	0.024
Cadillac DeVille	0.031	0.019	0.027	0.042	0.030	0.038	0.037	0.015	0.013	0.026
Toyota Celica	0.040	0.031	0.020	0.028	0.030	0.007	0.007	0.007	0.007	0.007
Acura MDX	0.005	0.005	0.005	0.007	0.006	0.031	0.027	0.007	0.007	0.018
Porsche 911	0.007	0.011	0.017	0.019	0.013	0.015	0.019	0.008	0.010	0.013
Mini Cooper	0.013	0.015	0.046	0.059	0.033	0.009	0.003	0.004	0.004	0.005
Honda S2000 CR	0.046	0.043	0.008	0.059	0.039	0.017	0.013	0.003	0.007	0.010
Grand Marquis	0.017	0.014	0.009	0.014	0.014	0.027	0.025	0.008	0.015	0.019
Nascar Cup Car	0.019	0.009	0.019	0.009	0.014	0.017	0.023	0.008	0.004	0.013
Fleet Average	0.024	0.020	0.022	0.029	0.024	0.019	0.019	0.009	0.010	0.019

Table 4.3: Average camber and toe of all test vehicles in normal control tests.

No. of Trials		Camber (degrees)				Toe (degrees)			
		LF	RF	LR	RR	LF	RF	LR	RR
79	Mercedes E320	-1.13	-1.22	-1.43	-1.80	0.09	0.09	0.10	0.14
20	Cadillac DeVille	0.00	-0.64	0.08	-0.16	0.06	0.08	0.05	0.02
10	Toyota Celica	-0.60	-1.07	-3.21	-2.94	-0.07	-0.10	0.14	0.13
10	Acura MDX	-0.48	-0.62	-1.19	-1.57	-0.05	-0.06	0.14	0.10
15	Porsche 911	-0.19	-0.47	-1.32	-1.33	-0.04	-0.05	0.08	0.16
10	Mini Cooper	-1.07	-1.78	-1.57	-1.77	0.20	0.20	0.08	0.21
10	Honda S2000 CR	-3.19	-3.10	-3.00	-2.65	0.04	0.03	0.01	0.06
21	Grand Marquis	-1.42	-1.24	-0.43	-0.42	0.07	0.04	0.00	-0.05
10	Nascar Cup Car	6.61	0.24	1.66	-1.52	0.29	0.27	-0.06	-0.66

We performed over 160 full wheel alignment measurements and concluded that the measurements are strongly affected by some variables tested, while some do not influence the measurements. However, the largest effects on wheel alignment accuracy that can be expected to arise in a plant or wheel alignment shop are caused by levelness of the platform and errors in tire pressure. For those doing wheel alignment studies, there is also the concern of ratcheting suspension inching a car forward into the bumpers.

In summary:

1. For accurate camber and toe measurements, it is important the bearing plates are level and coplanar.

2. For accurate measurements, it is important that wedge not be introduced by low tire pressures.

3. A single tire pressure error can have a stronger influence on the alignment results than even two diagonal tires being underinflated.

4. We measured no toe-in influence using a front lateral force pressure test up to 5kg.

5. We found that wheel alignment measurements changed very little over the fourteen months.

6. The reverse head results showed that variance is related more to fixturing than sensors, and that the number changes are small.

7. The repeatability of suspension alignment is not strongly affected by the softness of the suspension.

8. The wheel alignment measurements are influenced by the stiffness of the bushings.

9. Caution must be used with respect to the ratcheting effect on parked tires during repeated alignments of one vehicle.

4.3   A Word of Warning

One phenomena arose during the testing that would only show up in testing and not in normal use. We found that the rear suspension of a vehicle would ratchet forward when the vehicle was raised and then lowered. The impact was that if the transmission was left in park, the car would inch forward 6 mm (0.25) each time the car was raised and lowered. After several repeated measurements, we found that cars would be up against the front bumpers at the rear wheels. These bumpers are placed at the rear wheels to prevent a car from rolling off the bearing plates.

If the force was high enough against the bumpers, the rear suspension would generate tremendous friction and the rear camber would not be achieved because the tires were not supported completely by the bearing plates. In repeated measurements, it is important to assure that the rear tires are not bound up on the rear bearing plate bumpers.

4.4   Future Scope

The work presented in this research can serve as guidelines to perform wheel alignment measurements accurately. The pointers provided in conclusions can be followed by wheel alignment shops to eliminate errors caused due to operator or suspension variables. More in-depth research can be done on the influence of tire pressures on wheel alignment using different vehicles, and with stiff and soft suspensions. The effect of bushing stiffness on wheel alignment measurements can be further studied by replacing all the suspension bushings on the vehicle. It is certain that bushings have effects on wheel alignment angles, which is the reason why they are not preferred in motorsports (or use polyurethane bushings) due to their compliance effects. To sum it up, there is still some scope for this research in terms of suspension variables such as tire pressure and bushing stiffness which influence wheel alignment measurements.

BIBLIOGRAPHY

[1] Tkacik, P., Casino, M., Noakes, D., Kauffman, N., Rohwedder, D., Popat, J., Nabar, A., and Patel, H., "A Statistical Study of Operator Variables on Vehicle Wheel Alignment Measurements", 34th Tire Science and Technology Conference, Akron, OH, September 2015.

[2] Patel, H., Casino, M., Noakes, D., Kauffman, N., Rohwedder, D., Popat, J., Nabar, A., and Tkacik, P., "Suspension Variables Influencing Vehicle Wheel Alignment Measurements", Society of Automotive Engineers 2016 World Congress, Detroit, MI., April 2016.

[3] L. A. Fornasieri, J. P. Kushnerick, K. A. Freeman, D. F. Morgantini and R. J. Rivele, in Brakes, Steering and Suspension 1980-87, 1988, pp. 3-7.

[4] P. O. Aiyedun and B. O. Bolaji, "Automobile Engineering". (http://unaab.edu.ng/attachments/470_MCE%20504%20Automobile%20Engineering%20Web%20Note%20-%20Dr%20B%20O%20Bolaji.pdf)

[5] "Macpherson Strut" 2016. (http://en.wikipedia.org/wiki/MacPherson_strut)

[6] C. J. Longhurst, "The Suspension Bibles" 2016. (http://www.carbibles.com/suspension_bible.html)

[7] "Panhard rod" 2015. (https://en.wikipedia.org/wiki/Panhard_rod)

[8] "Watt's linkage" 2016. (https://en.wikipedia.org/wiki/Watt%27s_linkage)

[9] "Air suspension" 2016. (https://en.wikipedia.org/wiki/Air_suspension)

[10] Milliken, W. F., and Milliken, D. L. Race car vehicle dynamics. Vol. 400. Warrendale: Society of Automotive Engineers (1995).

[11] Powerflex GAC, "Suspension Geometry" 2016. (http://powerflexusa.com/suspensiongeometry.aspx)

[12] Dixon, J. C., Suspension Geometry and Computation, 2nd edition, 2009, John Wiley & Sons Ltd.

[13] Gillespie, T. D., Fundamentals of Vehicle Dynamics. Warrendale: Society of Automotive Engineers (1992).

[14] RIT Baja SAE, "Glossary of Suspension Terms". (http://edge.rit.edu/edge/RIT%20Mini-Baja/public/Glossary%20of%20 Suspension%20Terms)

[15] Viking Speed Shop, "Suspension 101 - Camber, Caster and Toe" 2016.
(http://www.vikingspeedshop.com/suspension-101-camber-caster-and-toe/)

[16] John. Hagerman, "Camber, Caster and Toe: What Do They Mean ?",
Smithees Race Car Technologies, 2016.
(http://www.ozebiz.com.au/racetech/theory/align.html)

[17] Nasada. M., "Effect on compliance and alignment variation with respect to
stiffness of knuckle and shock absorber in a McPherson strut suspension",
Vehicle System Dynamics: International Journal of Vehicle Mechanics and
Mobility, Volume 44, Supplement 1, 2006.

[18] Suh, N. M., Complexity: Theory and Applications, Oxford University, 2005.

[19] Ken W. Purdy, "Automobile", Encyclopedia Britanica, 2016.
(http://www.britannica.com/technology/automobile#ref527727)

[20] "Introduction to Suspension"
(http://www.thecartech.com/subjects/auto_eng2/INTRODUCTION_TO_SU
SPENSION.htm)

[21] "Suspension Tuning Cheat Sheet", Race Car Tuner, 2016.
(http://www.racecartuner.com/03/SuspensionCheatSheetV2.htm)

[22] "Articles about Handling", TurnFast!, 2016.
(http://www.turnfast.com/tech_handling/handling_springs)

[23] "Bushing (isolator)", Wikipedia, 2015.
(https://en.wikipedia.org/wiki/Bushing_(isolator))

[24] Drew. Taylor, "Rubber v/s Ployurethane Suspension Bushings", Diverse
Suspension Technologies, 2011.
(http://www.aftermarketsuspensionparts.com/blog/rubber-v-polyurethane-
suspension-bushings/)

[25] "Bushings: Urethane v/s Rubber", Speed Direct.
(http://www.speeddirect.com/index.php/tech-info/suspension-handling-
information/bushings-urethane-vs-rubber)

[26] "Suspension and Wheel Alignments", MileOne Collision Centers, 2016.
(http://www.mileonecollision.com/suspension-and-wheel-alignments/)

[27] "Different types of Alignment", Town Fair Tire.
(http://www.townfairtire.com/wheel-alignment/different-types-of-wheel-
alignments/)

[28] Vauderwange, T., Wheel Alignment, Vogel Buchverlag, 2011.

[29] "Watkins SmartStrings: Owner's Manual", Watkins Smart Racing Products.
(http://www.smartracingproducts.com/smartstrings/smartstrings_manual_v1.pdf)

[30] Hunter Engineering Company.
(http://www.hunter.com/)

[31] M. T. Stieff, "Vehicle Alignment Sensor System", US Patent No. 6,313,911 B1, 2001.

[32] M. T. Stieff, "Vehicle Alignment Sensor System", US Patent No. 6,483,577 B2, 2002.

[33] T. A. Strege, M. T. Stieff, N. J. Colarelli, III, "Microelectronic Vehicle Service System Sensor", US Patent No. 7,100,289 B1, 2006.

[34] R. W. Carter, R. E. Williams, "Method and Apparatus for Providing Runout Compensation in a Wheel", US Patent No. 5,052,111, 1991.

[35] J. D. Klarer, "Apparatus and Method for Maintaining Wheel Alignment Sensor Runout Compensation", US Patent No. 6,796,036 B1, 2004.

[36] "Operation Instructions: Pro-Align Wheel Alignment Systems", Hunter Engineering Company, 2009-2010.

[37] "12" Spirit Level 98Z-12 W/SLC Product Decription", L. S. Starrett, Athol, MA.
(http://www.starrett.com/metrology/product-detail/Levels/Machinsts-Levels/Precision-Hand-Tools/Precision-Measuring-Tools/98Z-12%20W SLC#Downloads.)

[38] Casino, M., Kauffman, N., Noakes, D., Rohwedder, D., "Vehicle Suspension Alignment Validation", University of North Carolina at Charlotte, 2015.

[39] "Instron Model 4400 Universal Testing Machine", 1995.
(http://fab.cba.mit.edu/content/tools/instron/M10-94400-1.pdf)